



## Changes in Gene Expression and Estrogen Receptor Cistrome in Mouse Liver Upon Acute E2 Treatment

Gaëlle Palierne, Aurelie J Fabre, Romain Solinhac, Christine Le Peron, Stéphane Avner, Françoise Lenfant, Coralie Fontaine, Gilles Salbert, Gilles Flouriot, Jean-François Arnal, et al.

### ► To cite this version:

Gaëlle Palierne, Aurelie J Fabre, Romain Solinhac, Christine Le Peron, Stéphane Avner, et al.. Changes in Gene Expression and Estrogen Receptor Cistrome in Mouse Liver Upon Acute E2 Treatment. *Molecular Endocrinology -Baltimore-*, 2016, 30 (7), pp.709-732. 10.1210/me.2015-1311 . hal-01357623

**HAL Id: hal-01357623**

**<https://hal-univ-rennes1.archives-ouvertes.fr/hal-01357623>**

Submitted on 26 Sep 2016

**HAL** is a multi-disciplinary open access archive for the deposit and dissemination of scientific research documents, whether they are published or not. The documents may come from teaching and research institutions in France or abroad, or from public or private research centers.

L'archive ouverte pluridisciplinaire **HAL**, est destinée au dépôt et à la diffusion de documents scientifiques de niveau recherche, publiés ou non, émanant des établissements d'enseignement et de recherche français ou étrangers, des laboratoires publics ou privés.

# RESEARCH RESOURCE: Changes in gene expression and Estrogen Receptor cistrome in mouse liver upon acute E2 treatment

Gaëlle Palierne<sup>1,#</sup>, Aurélie Fabre<sup>2,#</sup>, Romain Solinhac<sup>2</sup>, Christine Le Péron<sup>1</sup>, Stéphane Avner<sup>1</sup>,  
Françoise Lenfant<sup>2</sup>, Coralie Fontaine<sup>2</sup>, Gilles Salbert<sup>1</sup>, Gilles Flouriot<sup>3</sup>, Jean-François Arnal<sup>2</sup>, Raphaël  
Métivier<sup>1</sup>.

<sup>1</sup> Equipe SP@RTE (Spatio-Temporal Regulation of Transcription in Eukaryotes), UMR 6290 CNRS  
(Institut de Génétique et Développement de Rennes), Université de Rennes 1. Campus de Beaulieu,  
Rennes, 35042 Cedex, France

<sup>2</sup> Equipe 9 « Estrogen receptor : *in vivo* dissection and modulation », INSERM U1048 (Institut des  
Maladies Métaboliques et Cardiovasculaires), Toulouse, 31432 Cedex 4, France

<sup>3</sup> Equipe TREC (Transcription, Environment and Cancer), INSERM U1085-IRSET (Institut de  
Recherche en Santé, Environnement et Travail), Rennes, 35042 Cedex, France

# Footnote. The first two authors should be regarded as joint First Authors.

**Abbreviated Title:** Estrogen-sensitive genome response of liver

**Key terms:** Estrogen, estrogen receptor, liver, mouse, transcriptome, cistrome, ChIP-seq

**Word count:** 9,503

**Number of figures and tables:** 11 Figures and 4 Tables.

*Corresponding author and person to whom reprint request should be addressed:*

Raphaël Métivier, PhD

Equipe SP@RTE. UMR CNRS 6290. Université de Rennes 1. Rennes, 35042 Cedex, France.

Phone: 33 (0)2 2323 5142

Fax: +33 (0)2 2323 6794

Email: [raphael.metivier@univ-rennes1.fr](mailto:raphael.metivier@univ-rennes1.fr)

**Disclosure Statement:** The authors have nothing to disclose.

## Abstract

Transcriptional regulation by the Estrogen Receptor  $\alpha$  (ER) has been investigated mainly in breast cancer cell lines but estrogens such as 17 $\beta$ -Estradiol (E2) exert numerous extra-reproductive effects, particularly in the liver where E2 exhibits both protective metabolic and deleterious thrombotic actions. To analyze the direct and early transcriptional effects of estrogens in the liver, we determined the E2-sensitive transcriptome and ER cistrome in mice following acute administration of E2 or placebo. These analyses revealed the early induction of genes involved in lipid metabolism, which fits with the crucial role of ER in the prevention of liver steatosis. Characterization of the chromatin state of ER binding sites (BSs) in mice expressing or not ER demonstrated that ER is not required *per se* for the establishment and/or maintenance of chromatin modifications at the majority of its BSs. This is presumably a consequence of a strong overlap between ER and Hepatocyte nuclear factor 4  $\alpha$  (Hnf4 $\alpha$ ) BSs. In contrast, 40% of the BSs of the pioneer factor Foxa2 were dependent upon ER expression, and ER expression also affected the distribution of nucleosomes harboring dimethylated H3K4 around Foxa2 BSs. We finally show that, in addition to a network of liver-specific transcription factors including Cebp $\alpha/\beta$  and Hnf4 $\alpha$ , ER might be required for proper Foxa2 function in this tissue.

## Introduction

Estrogen receptors (Esr1: ER $\alpha$ , termed ER throughout the manuscript; and Esr2: ER $\beta$ ) are ligand-dependent transcription factors that mediate the effects of estrogens such as 17- $\beta$  estradiol (E2) (1,2). Estrogens control the development, differentiation and function of tissues involved in reproduction, but are also pleiotropic hormones controlling the metabolism and homeostasis of many other tissues. They can be harmful or beneficial according to the target tissue, with deleterious effects in the development of cancers of uterus and breast, but protective effects on the bones, arteries and metabolism since they reduce the incidence of osteoporosis, atheroma, and type 2 diabetes (3).

The molecular actions of ER have been extensively studied *in vitro* in human cell lines, using mostly the prototypical breast cancer cell line, MCF-7. Over the last decade, genome-wide analyses obtained from such *in vitro* models have greatly challenged the historical view of proximal ER-directed gene regulation (4-6) and it is now accepted that, in breast cancer cells, ER can dynamically engage between 15,000 and 30,000 binding sites (ER BSs) across the genome. Once tethered to chromatin at these sequences, ER regulates transcription of its target genes through the dynamic recruitment of multiple partners including cofactors of diverse families of proteins and components of the transcriptional machinery (7-10). Importantly, most of the ER BSs that have been determined so far are thought to be enhancers located away from the transcriptional start site (TSS) of annotated E2-sensitive genes (11,12), although transcription of so-called enhancer RNAs (eRNAs) could occur at these places (13,14). The actions of pioneer TFs have also been demonstrated genome-wide as essential for the accuracy and frequency of ER binding. FOXA1 is one of the most studied of these proteins (6,11,15). It can bind to condensed chromatin to prepare it for the subsequent recruitment of other TFs, presumably by acting as a recruitment platform for histone modification and/or nucleosome remodelling complexes (16-18).

Whether these mechanisms actually apply *in vivo* remains uncertain and requires careful attention. Genome-wide analysis of the ER cistrome in tissue explants from normal human mammary glands has demonstrated that ER binding events in these differentiated primary cells are much more restricted than those in cancer cell lines (19). In addition, although ERs and FOXA have been shown to cooperate in establishing the estrogen-dependent protection of the liver against hepatocellular

carcinoma (20,21), the nucleosome positions and chromatin structure around Foxa sites were also found to be independent of Foxa1 and Foxa2 expression in differentiated adult mouse liver (22). This leads one to wonder whether Foxa proteins do indeed exert a pioneering influence on ER activity and whether they use similar mechanisms in the liver as those in human mammary gland.

As well as establishing these mechanistic aspects of ER function *in vivo*, studying the actions of E2 in the liver *in vivo* is also of utmost physiological interest since estrogens play important protective and deleterious roles. For example, E2 directly contributes to liver protection from the deleterious consequences of metabolic stresses such as a High Fat Diet (HFD) since it prevents HFD-induced liver steatosis through the activation of hepatocyte ER (23,24). On the other hand, exogenous estrogens administered for oral contraception or hormone replacement therapy at menopause stimulate the production of angiotensinogen, sex hormone-binding globulin and circulating hepatic coagulation factors (25). These changes are greatly enhanced by the oral route due to hepatic first-pass and appear to contribute, at least in part, to an increased risk of venous thrombosis and its life-threatening complication, the pulmonary embolism (26). It is thus of major interest to describe and understand the mechanisms of action of estrogen in the liver, since this organ represents an important target for these hormones and can mediate both the desired (protection against liver steatosis) and deleterious (contribution to increased risk of venous thrombosis) actions of estrogens. However, so far the estrogen-sensitive liver transcriptome and the ER cistrome have been characterized only under chronic hormonal treatment (20,27-29).

Given this, we aimed to decipher the early steps of the mechanisms engaged by ER at the chromatin level that control liver gene expression following acute administration of E2 *in vivo*. To differentiate between ER-dependent and ER-independent processes, and to understand chromatin events induced by an ER deficiency, we gathered data from wild-type or ER knock-out (ERKO) mouse livers. Here, we demonstrate that although the liver transcriptional response to E2 is fully dependent upon ER expression, an ER deficiency has no drastic consequences on enhancer chromatin signatures. However, we provide evidence that ER is required for Foxa2 binding at a subset of sites, and that a network of other TFs may protect Foxa2 sites from loss of chromatin functionality.

## Materials and Methods

### Ethics statement

All procedures involving experimental animals were performed in accordance with the principles and guidelines established by the “Institut National de la Santé et de la Recherche Médicale” (INSERM) and were approved by the local Animal Care and Use Committee.

### Mice

ER-null mice (ERKO) from a C57BL/6 genetic background were generated as previously described (30) and were kindly provided by Prof P Chambon (Strasbourg, France). Female wild-type (ERWT) and ERKO mice littermates were obtained from the same parents. Mice were housed in groups of 5 per cage and kept in a temperature-controlled facility on an artificial 12h light-dark cycle. Genotyping was systematically performed on DNA prepared from tail biopsies using a mix of specific primers P4 (intron 1): 5'-GCTTTCCTGAAGACCTTTCATATGGTG-3', P3 (antisense in intron 2): 5'-GGCATTACCACTTCTCCTGGGAGTCT-3', and mESR1ex2: 5'-CAATCGACGCCAGAATGGCCGAG-3'. Mice were ovariectomized at 4 weeks of age and then treated by oral gavage with placebo (castor oil, 5% ethanol) or E2 (1 mg/kg) at 10 weeks of age. Following anesthesia by intraperitoneal injection of ketamine (100 mg/kg) and xylazine (10 mg/kg), mice were sacrificed 1 or 4 hours after gavage. Blood was collected by retroorbital puncture and livers were used immediately or snap-frozen in liquid nitrogen and stored at -80°C.

### RNA preparation

Ovariectomized ERWT or ERKO mice were treated or not with E2 for 4 hours. Following the extraction of livers and tissue homogenization using a Precellys tissue homogenizer (Bertin Technology), total RNAs were prepared using GenElute Mammalian Total RNA Miniprep Kit (Sigma-Aldrich). For Rt-qPCR experiments, 1 µg total RNA was reverse transcribed using a High Capacity cDNA Reverse Transcription Kit (Applied Biosystems) and subjected to qPCR.

### Gene expression arrays

We used the One-Color Quick Amp Labeling kit (Agilent) to synthesize and label cRNAs using 200 µg RNA, according to the manufacturer's instructions. 600 ng Cy3-labelled cRNA were

hybridized to a SurePrint G3 Mouse GE microarray (8X60K) at the GeT-TRIX Genopole facility (Toulouse, France). Slides were scanned immediately and data were analyzed with Feature Extraction Software 10.10.1.1 (Agilent) using the default parameters. All subsequent analyses were done under R (www.r-project.org) using packages of Bioconductor (www.bioconductor.org). We used the limma package for data normalization, selecting spots with a weight of one in at least three arrays from at least one experimental group, and carried out normalization using the quantile method. Experimental groups were compared by analysis of variances (*t*-test) and *p*-values were adjusted by the Benjamini and Hochberg (BH) method. Genes were considered as differentially expressed between two experimental conditions when their adjusted *p*-value was lower than 0.05 and their fold change greater than 1.5. The lists of all significantly regulated genes are given in **Supplemental File 1**. Functional annotations were performed under the web-platform webgestalt (<http://bioinfo.vanderbilt.edu/webgestalt/>) (31). Enrichments were calculated over the genome reference, using a BH-corrected *p*-value<0.0001 and considering only categories including at least 3 genes. Comparative analysis with publicly-available datasets at the NCBI's Gene Expression Omnibus website (<http://www.ncbi.nlm.nih.gov/geo/>) (32) used the generated lists of genes from GSE57804 (33), GSE13265 (27), GSE45346 (28), GSE36514 (29) and GSE23850 for human MCF-7 (34).

#### **MeDIP and hMeDIP assays**

Immunoprecipitation of methylated or hydroxymethylated cytosines (MeDIP or hMeDIP, respectively) were performed as described previously (35) on liver genomic DNA prepared using the DNeasy Blood Tissue Kit (Qiagen). We used 5 µg genomic DNA and 2 µg anti-5mC antibody or 15 µg DNA and 5 µg anti 5-hmC antibody for MeDIP or hMeDIP, respectively. Immunoprecipitated DNA was purified *via* standard phenol-chloroform and ethanol precipitation procedures, and resuspended in 100 µl TE. Two µl of these samples were used for qPCR reactions.

#### **ChIP experiments**

Livers were extracted from animals 1 hour after oral administration of placebo or E2, then sliced into small pieces and disrupted in 5 ml PBS by pressure through a 21G syringe needle. Cells from one half of a liver were fixed in 10 ml PBS containing 1% formaldehyde for 10 min at room temperature. Cross-linking was then stopped by incubation with 0.125M glycine at room temperature. Cells were

washed twice with PBS and then lysed in 1 ml buffer [10 mM Tris-HCl (pH 8.0), 10 mM NaCl, 3 mM MgCl<sub>2</sub>, 0.5% Igepal] containing 1X protease inhibitors (Complete Inhibitors, Roche). Extraction of nuclei was then performed by applying 50 strokes of potter on the suspension in an ice-cold Dounce followed by further incubation for 5 min at 4°C. Nuclei suspensions were then centrifuged at 13,000 rpm at 4°C. Following two washes in PBS, nuclei were lysed by incubation in 4 ml lysis buffer [10 mM EDTA, 50 mM Tris-HCl (pH 8.0), 1% SDS, 0.5% Empigen BB (Sigma)] on ice for 10 min and sonification using a Branson 250 apparatus (3 pulses of 20 sec at 50% power, with at least 1 min on ice between each pulse). SDS was then neutralized by addition of 400 µl 10% Triton X-100 and chromatin was further sonicated by two additional 14 min sonications of the lysed nuclei in a BioRuptor apparatus (Diagenode) operating at high intensity with 30 sec on/off duty cycles. Chromatin was then cleared by a 10 min centrifugation at 10,000 x g and the supernatants were pooled for further use. ChIP experiments were performed using 300 µl of these chromatin preparations and 2 µg antibodies (**Supplemental Table 1**), as previously described (34,35). DNA was purified on NucleoSpin™ columns (Macherey-Nagel) using NTB buffer. Subsequent qPCR analysis used 2 µl of 5-fold diluted input material and 2 µl of ChIP samples.

#### **ChIP-seq**

All ChIP-seq were performed on livers from the same 5 individuals per genotype and treatment groups. We pooled DNA originating from 20 different ChIP experiments performed as described above, *i.e.* 4 ChIP experiments per mouse. Construction of libraries and sequencing using an Illumina HiSeq apparatus were conducted at the IGBMC sequencing facility (Strasbourg, France). Reads were aligned onto the indexed chromosomes of the mm9 genome using bowtie 0.12.7 (36) with parameters allowing at most two mismatches, and selected for unique mapping onto the genome. Sequencing statistics are given in **Supplemental Table 2**. Due to the small amounts of recovered DNA in the ER ChIP experiments performed on livers from placebo and E2-treated ovariectomized animals, we combined reads obtained in two runs of sequencing to reach a representative sequencing depth. Extracted reads were converted to .wig signal files using samtools 0.1.12a (37) and MACS 1.4.1 (38) with default parameters. To minimize the bias of diverging sequencing depths between different samples immunoprecipitated with the same antibody, the signal intensities of a given .wig were



normalized so as to be comparable to the .wig file with the highest sequencing depth. Peak callings were then performed as described in (35) with different  $p$ -values and peaks defined as being constituted of at least 4 adjacent signals within 65 bp above the threshold values. Peak callings for histone marks ChIP-seq were done with a stringent  $p$ -value =  $1e^{-12}$ . All repetitive sequences were eliminated from the identified genomic regions using lists obtained from the UCSC (blacklist; <http://genome.ucsc.edu/cgi-bin>). Bed files corresponding to the genomic coordinates of identified ER BSs and Foxa2 BSs are given in **Supplemental File 2**. Motif analysis was performed using the CentDist algorithms (<http://biogpu.ddns.comp.nus.edu.sg/~chipseq/webseqtools2>) and SeqPos tool on the cistrome web-platform (<http://cistrome.org/ap/>) (39), and illustrated within Wordles pictures (<http://www.wordle.net/>). For SeqPos analyses, we restricted the analyses to the top 5,000 sites when required, as defined by their maximum mean intensity in a 1 kb window centered on each region. When required Sequences were declared enriched with a  $p$ -value < 0.05 and Z-score > 2.5. All integrative analyses of the ChIP-seq data were performed using home-made scripts and algorithms from the cistrome web-platform. Analysis of publicly-available fastq ER ChIP-seq data at the GEO (32) or Array Express (<http://www.ebi.ac.uk/arrayexpress/>) (40) websites were performed under the same conditions. ER datasets analyzed were the GSE52351 (33), GSE36455 (41), E-MTAB-805 (20) and GSE25021 (42) for MCF-7 cells. Genomic regions identified by ChIP-chip assays (43) were extracted from the supplemental material of the manuscript and converted from mm5 to mm9 genome annotation. The .bed files corresponding to the cistromes of other transcription factors were all obtained from the cistrome finder system (<http://cistrome.org/finder/>; 44,45): Foxa1 (GSM427090; 46), Cebp $\alpha$  (GSM548908; 47), Cebp $\beta$  (GSM427088; 46), Ppara (GSM864671; 48), Rxra (GSM864674; 48), GR (common peaks from replicates GSM1122512 and GSM1122515; 49), Esrra (GSM1067408; 50), NR1D1 (GSM647029; 51), NR1D2 (GSM840529; 52), HDAC3 (common peaks from replicates GSM647022, GSM647023 and GSM647024; 51), NCor1 (GSM647027; 51), CTCF (GSM722759; 53) excepting Hnf4a (GSE57807; 54) and NKx3-1 (common peaks from duplicate GSM878195 and GSM878196; 55) data, which were re-analyzed with our scripts.

## **Real-time PCR (qPCR) and statistics**

Sequences of all oligonucleotides used in this study are given in **Supplemental Table 3** (RNAs) and **Supplemental Table 4** (ChIPs). Oligonucleotides for RT-qPCR were designed using NCBI/Primer-Blast (<http://www.ncbi.nlm.nih.gov/tools/primer-blast/>). All other primers were designed using the Primer3 program (<http://frodo.wi.mit.edu/primer3/>) (56). All ChIP-qPCR experiments were carried out using a BioRad MyiQ apparatus with 1  $\mu$ M oligonucleotide and a BioRad iQ SYBR Green supermix with 50 rounds of amplification followed by determination of melting curves. RT-qPCRs were performed on 96.96 Dynamic Arrays for the microfluidic BioMark system (Fluidigm Corporation) or using an ABI ViiA 7 apparatus. All statistical analyses of qPCR data were performed using GraphPad<sup>TM</sup> Prism software. Mann-Whitney non-parametric *t*-tests were used to determine significant variations from controls. Heatmaps of expression values and qPCR data were all generated using MeV (57). To normalize the data obtained from microarray experiments into a similar dynamic range, expression values shown within the heatmaps were normalized per mRNA as Normalized value= [(Value) – Mean(Row)]/[Standard deviation(Row)].

## Data deposition

The microarray and ChIP-seq data generated in this study have been submitted to the NCBI Gene Expression Omnibus website (<http://www.ncbi.nlm.nih.gov/geo/>) (32) under accession No. GSE70350.

## Results

### Establishment of E2- and ER-dependent transcriptomes in liver

Estrous cycle-dependent (58) or estrogen-sensitive transcriptomes in harvested livers (33) or in native animals treated by chronic administration of hormones (27,28) have already been documented. Here, we aimed to characterize the ER-dependent mechanisms of transcription regulation in the liver *in vivo* and to correlate these data with data on ER binding to chromatin at shorter times of treatment. Therefore, we chose to treat ovariectomized female ER<sup>+/+</sup> (ERWT) and their ER<sup>-/-</sup> (ERKO) littermate mice through gavage with E2 or placebo (P) for 4 hours, in castor oil solution. These conditions were deliberately chosen in order to engage the hepatic first-pass which is likely to have a

role in E2-induced venous thrombosis (26), as opposed to transcutaneous hormone injections. Liver mRNAs from ERWT or ERKO mice treated or not with E2 in these experimental conditions were then isolated and microarray analysis was performed. Differentially expressed genes between two conditions were considered significant when their fold change in expression were  $>1.5$  with an adjusted  $p$ -value of  $<0.05$ . The list of all significantly regulated genes is given within **Supplemental File 1**. Despite a relatively elevated inter-individual variation in gene expression levels (**Fig. 1A**), these analyses were able to identify 124 E2-regulated mRNAs in ERWT, which corresponded to 110 unambiguously annotated unique genes (**Fig. 1B**). Importantly, in ERKO animals, the E2 treatment did not significantly affect the transcriptional regulation of any genes (**Supplemental Fig. 1**). This result confirms that ER is required for the response of all of the identified genes to an acute treatment with E2. Approximately 80 % of the identified genes in ERWT mice were up-regulated by E2 (**Fig. 1A**) and were grouped into functional annotations relevant for lipid and alcohol metabolisms, growth factor signalling and other functional pathways specific of the liver (**Table 1**). Interestingly, although performed in different experimental settings, 48 (44%) of the identified E2-sensitive genes here were similar to those determined previously following 3 days of treatment with the ER agonist PPT {4,4',4''-(4-propyl-[1H]-pyrazole-1,3,5-triyl)trisphenol} (28) (**Supplemental Fig. 2**). Our data also identified 194 mRNAs (129 genes) whose expressions were significantly different in ERKO compared to ERWT mice in the absence of E2 treatment (**Fig. 1A and 1B**). The ER coding gene *Esr1* was included in these 129 genes, thereby validating our analyses. These ER-dependent genes were identified as involved in cell growth/differentiation but also in lipid metabolic processes and mammary gland development (**Table 1**). Independent RT-qPCR experiments confirmed the observed changes in regulation for 91% of the 45 tested E2-regulated genes and 41.7% of the 12 tested ER-dependent genes (**Supplemental Fig. 3**). As illustrated within the Venn diagram depicted in **Fig. 1B**, only 10 of the ER-dependent and E2-sensitive genes also exhibited an ER-dependent basal expression. This may indicate that the remaining 119 genes with an ER-dependent basal expression are regulated by E2 (or other endogenous estrogens/signals) under different conditions of time or diet than those used in our analyses. The differential expression of these 119 genes in livers from ERKO vs. ERWT mice could also be an indirect consequence of ER gene inactivation in liver, whereby

dysregulation of one or more of these genes may provoke the observed effects. However, only a small proportion of the ER-dependent genes found here are similar to those reported by another study performed in mice with liver-specific ablation of *Esr1* expression (29). So it is possible that the changes in gene expression that we observed here between ERWT and ERKO livers are due to alterations of the function of (an)other tissue(s).

#### Identification of ER binding sites in liver

To determine whether ER is a direct transcriptional regulator of the E2- and/or ER-sensitive transcriptomes identified above, and to obtain mechanistic insights into these regulations, we next established the cistrome of ER in placebo and E2-treated livers. In particular, we aimed to determine whether ER is bound to chromatin in the absence of E2, as has been reported in cultured cancer cells (59-62). Indeed, ER cistromes have already been determined for mouse liver by ChIP-chip (43,58) or ChIP-seq methods in intact (20) or harvested liver cells (33), however these have not been carried out in the absence of E2. Hence, we conducted ChIP-seq experiments to establish the cistrome of ER in livers from ovariectomized E2- or placebo- (P) treated wild-type mice. We used chromatin prepared from livers of ovariectomized E2-treated ERKO individuals as a control. To reduce any cistrome variation due to individual animal specificities, we pooled and sequenced the DNA fragments purified from ChIP experiments performed on chromatin prepared from five different animals. Sequenced reads were aligned onto the genome and enriched regions were identified at different  $p$ -values (Fig. 2A). To determine the appropriate threshold enabling a comparison between the different cistromes, we calculated their overlap with decreasing significance (Fig. 2B). As expected, the overlap between two sets of genomic regions paralleled the threshold stringency. For instance, at a  $p$ -value of  $10^{-15}$ , 80% of the 87 ER BSs identified in placebo-treated ERWT animals were common with the 948 identified in E2-treated ERWT mice. In all subsequent analyses, we used ER cistromes determined with a  $10^{-5}$   $p$ -value threshold, which constituted the inflexion point for all overlapping ER BSs determined under the different conditions. At this threshold value, 3,857 ER BSs were identified in livers from E2-treated ERWT animals, 857 under control conditions, and 54 in ERKO (Fig. 2C). Using a similar approach we also confirmed that the ER cistromes from the liver overlap poorly with those reported

for the aorta and uterus (**Supplemental Fig. 4**) (33,41). Interestingly, 476 ER BSs detected in placebo-treated ERWT mice were not identified in E2-treated samples. Surprisingly, 14 additional regions were declared as specific to ERKO livers (**Fig. 2C**). Heatmaps of ChIP-seq binding values (**Fig. 2D**) as well as mean binding values (**Fig. 2E**) confirmed the presence of an ERKO-specific signal at these genomic regions (sub-panel #2 in **Fig. 2D**), indicating that these 14 BSs were likely not generated by a peak-calling approximation. These graphs also confirmed the specific binding of ER in ERWT livers either treated with E2 or placebo on corresponding ER BSs. This demonstrates that the placebo-specific ER BSs are not indicative of a residual binding of ER on the strongest sites observed in E2-treated livers. Finally, we observed that ER binding to the 345 ER BSs identified in placebo and E2-treated livers from ERWT animals was enhanced in hormone-stimulated conditions (**Fig. 2E**).

### Examination of ERKO and placebo-specific ER BSs

To validate the conclusions that could be made from our ChIP-seq data, we used qPCR to analyse ER binding to genomic regions presumed to either (i) bind ER in ERWT animals in both presence or absence of E2 (series #1); (ii) specifically recruit ER placebo-treated ERWT mice (series #3); or (iii) bind an ER-like protein in ERKO mice (series #2). We also took five randomly chosen sequences that did not recruit ER (#0 regions). The heatmaps in **Fig. 3** summarize the results of these experiments (mean data and statistics are shown in **Supplemental Fig. 5**) which were performed on ChIP samples prepared from four mouse livers (numbers on the top of the panel) that differed from those processed for ChIP-seq to generate independent data. A fraction of the pool of DNA that was subjected to high-throughput sequencing (HTS) served as a control. The promoter of the *Rplp0* gene was used as a normalizing ER-negative region, and two genomic regions located at the vicinity of the E2-regulated *Gdf15* gene were used as controls: one mobilized ER (Gdf15.3) and one did not (Gdf15.2). The results of these experiments confirmed the expected binding of ER to ER BSs from the #1 series of genomic regions, and not to those from the #0 series (**Fig. 3A**, left side of the panel). Moreover, these data showed an elevated level of variation concerning the binding of ER to the #2 and #3 regions detected in the different samples. For instance, in only two of the samples (one being the HTS sample), a protein recognized by the antibody used in these assays was specifically recruited (enrichment>2) to

four of the five tested #2 regions supposedly specific for ERKO livers. These observations led us to hypothesize that the antibodies targeting the C-terminal region of ER used for the ChIP-seq may purify a small number of non-specific genomic targets. High variations in enrichment levels were also evidenced between the five samples in the case of the ERWT placebo-specific ER BSs. Hence, we performed ChIP-qPCR assays with a specific antibody directed against the N-terminal region of ER on the same preparations of chromatin. As shown within the heatmap on the right side of the **Fig. 3A** (mean data and statistics are provided in **Supplemental Fig. 5**), whilst we were able to validate the binding of ER to the #1 series of genomic regions using this different antibody, this was not the case on the ERKO-specific ER BSs (#2 sites). These data indicated that the ER binding sites detected in ERKO mice may have represented a false-positive background of the ChIP-seq experiments, due either to the antibody or the pipeline used for processing the sequencing tags. Furthermore, as shown in **Table 2**, no specific motif related to an ER binding could be detected in ERKO sites, contrasting with the classical sequences found in the ER BSs identified in ERWT mice, such as FOX, HNF4, SP1 and AP1/AP2 motifs (full motif analysis is provided within the **Supplemental Fig. 6** and **Supplemental File 3**). ERKO sites were therefore excluded from the subsequent analyses described in this manuscript. Likewise, the results obtained from these ChIP-qPCR experiments performed with the N-terminal antibody did not validate any of the 5 tested ER BSs specific for placebo-treated ERWT livers (compare the results obtained for the #3 series of genomic regions on left and right sides of **Fig. 3A**). This indicated that either none of the ER BSs falling in this placebo-specific category constitute actual sites of ER binding or that these sites may be subjected to extreme inter-individual variation. Hence, we conducted ChIP-qPCR on 14 more genomic regions of this #3 category using liver chromatin prepared from additional animals (5 treated with placebo and 3 with E2). Results of these experiments, illustrated within **Fig. 3B**, showed that 2 of these 14 sites (#3.18 and #3.19) were not detected in these independent experiments using the anti C-terminal antibody and that 5 (#3.7, #3.11, #3.17, #3.20 and #3.21) of the remaining 12 ERBSs were enriched in the DNA fractions enriched with the anti-N-terminal antibody.

In conclusion, as in human cancer cells, a mobilization of ER on chromatin can be detected in the absence of ligand in livers from ovariectomized mice. The existence of genuine placebo-only sites

was also confirmed in our ChIP-qPCR experiments. However, their number, as determined from our ChIP-seq data, may be biased or even overestimated *i)* because of the use of a C-terminal antibody that can generate false-positive regions with low-level of enrichments (such as the 54 ERKO sites); and/or *ii)* because the N-terminal epitope targeted by the antibody used in our confirmation ChIP-qPCR experiments is not accessible for chromatin-bound ER in placebo conditions.

#### **ER BSs are “enriched” in the proximity of liver-specific genes**

Interestingly, in E2- and placebo-treated animals, 14.5% and 12.9% of the identified ER BSs respectively were found at a short distance (<3kb) from the promoters of annotated genes (**Fig. 4A**). When compared to the ER cistromes determined for human breast cancer cells, such an enrichment was clearly different from those identified for ER in the liver, uterus and, albeit to a lower extent, the aorta (**Fig. 4B** and **Supplemental Fig. 7**). Indeed, in E2-treated MCF-7 breast cancer cells, only 2 to 4% of the ER BSs identified were located in the vicinity of gene promoters (<3kb) (**Fig. 4B**). Note that an additional hour of treatment of mouse with E2 (2 hours in total) did not affect the distribution of ER BSs across the genome (data not shown). Importantly, GREAT (63) functional annotation of the ER cistrome in the liver also indicated that genes located proximal to and/or in relation to the identified ER BSs were clearly associated with liver-specific expression, function and diseases, such as lipid homeostasis and responses to insulin (**Table 3**). These data showed that the E2-mediated regulation of the rate of gene transcription in mouse liver may involve more proximal mechanisms than in human cancer cell lines, *i.e.* through binding of ER and its coregulators in the vicinity of the TSS. This hypothesis was confirmed by the observation that 28% of liver E2-regulated genes exhibited at least one ER BS within a 0-5kb window around their TSS, compared to 13% in MCF-7 cells (**Fig. 4C**). Interestingly, 75% of the genes characterized by an ER-dependent basal expression were located at distances >25kb from any ER BS (**Fig. 4C**). Again, this may reflect either an indirect effect of ER loss on the transcriptional rate of these particular genes, or their preferential long-range regulation. Finally, apart from a slight increase for genes within a 1-5 kb window, the strength of gene regulation by E2 could not be correlated with the distance between their TSS and the ER BSs neither in mouse liver nor MCF-7 cell lines (**Fig. 4D**).



### **ER loss impacts the chromatin status of the promoters of its target genes**

A loss of ER binding at some genomic regions could be either the source or a consequence of drastic changes in chromatin structure at these sites, including post-translational modifications of histones and DNA modifications. The nucleosomes located in active regulatory elements like enhancers exhibit histone marks such as H3K4me1, H3K4me2 and H3K27ac (64-66), and their DNA is globally characterized by low levels of CpG methylation that is inversely correlated to their hydroxymethylation status (35,67,68). Thus, we performed ChIP-seq experiments that aimed to determine the genome-wide location of nucleosomes marked with the H3K27ac or H3K4me2 modifications. As shown within **Fig. 5A**, the mean enrichment of these two marks around ER BSs (as defined by the sum of ER BSs detected in placebo- and E2-treated animals) exhibited biphasic curves around the center of the ER BSs, reflecting the existence of modified nucleosomes surrounding poised/activated genomic regions (69-72). Importantly, the relative enrichment of ER BSs in H3K4me2 and H3K27ac were relatively similar in ERWT and ERKO mice (**Fig. 5B**). Furthermore, less than 3% of the ERBSs were overlapping with either the 4,084 or 2,137 genomic regions losing their H3K4me2 or H3K27ac marks in ERKO livers (**Supplementary Fig. 8**). This suggested that the binding of ER to its sites is not required for the establishment and/or maintenance of these chromatin modifications. Note that the presence of the two chromatin marks H3K4me2/H3K27ac slightly but significantly decreased at the promoter regions of genes transcriptionally down-regulated in ERKO livers (**Fig. 5C**), and conversely increased in the promoters of up-regulated ones. Interestingly, variations in H3K4me2 and H3K27ac contents were more coordinated in the promoters of up-regulated genes than in those of down-regulated genes (**Fig. 5D**). This indicates that the promoter regions of genes undergoing a “gain of function” in ERKO livers may be subjected to stronger chromatin remodelling than genes with a reduced transcriptional activity in ERKO.

### **Hnf4 $\alpha$ may protect ERBSs from losing their chromatin functional state in ERKO liver**

In order to examine the possibility that some variations of chromatin functionality could occur in a specific sub-population of ER BSs, we clustered the profiles of H3K4me2 and H3K27ac modifications around these genomic regions (heatmaps of ChIP-seq signals in **Fig. 6A**). With the exception of the ER BSs classified within clusters 7, 9 and possibly 4 (mean signals are shown in **Fig.**



**6B**), no variations in H3K4me2 signals were apparent in ERKO compared to ERWT mice. Interestingly, in these two/three cases the enrichment levels of ER BSs in H3K4me2 did not significantly differ but the shape of the curves shifted from biphasic to monophasic shapes (see enlarged view in the corresponding panels). A similar shift was also observed in the case of the cluster 4, but to a slighter extent. This suggests that the ER BSs included within clusters 7, 9 and possibly 4 were changing their functionality/poised state. However, we did not observe any variations in H3K27ac levels in these clusters (**Supplemental Fig. 9**), indicating that this loss in functionality may only affect the stability and/or the presence of an H3K4me2-marked nucleosome at the center of the ER BS.

To validate these genome-wide observations and give further details on the exact loss of functionality of ER BSs in ERKO mice, we next evaluated the enrichment of ten ER BSs with H3K4me1, H3K4me2 and H3K27ac by ChIP-qPCRs using chromatin prepared from the same E2-treated ERWT and ERKO animals as previously described. The results of these experiments (data and statistics in **Supplemental Fig. 10**) are illustrated as heatmaps of enrichment in **Fig. 7A**. These data indicate that the presence of mono- or di-methylated H3K4 around the 10 tested ER BSs was not drastically affected in ERKO livers when compared to ERWT ones. The same results were observed for their K27 acetylation status. However, interestingly, in ERKO mice a small but significant increase in both H3K4me1 and me2 content was observed at the #1.3 ER BS, and an increase in H3K4me2 was seen at the #3.1 ER BS. These small increases in H3 modifications may be in accordance with the fact that, on some ER BSs, the shift from biphasic to monophasic shapes of enrichment observed by ChIP-seq actually reflects a more stable central H3K4me2-marked nucleosome. Finally, we envisioned that increased amounts of 5-mC or a decreased presence of 5-hmC on enhancer DNA may have accounted for the observed loss of functionality of ER BSs in ERKO mice. To test this hypothesis, we performed (hydroxy-) methylated DNA immunoprecipitation experiments (abbreviated to MeDIP and hMeDIP) and evaluated the enrichment of sites of interest of these two modified bases using qPCR. The results of these assays (**Supplemental Fig. 10**, summarized in **Fig. 7B**) indicated that the 10 tested enhancers were poorly enriched in 5-mC, and that the loss of ER had no general impact on these levels, apart from a slight but not significant increase in

the #1.2 ER BS in ERKO mice. In most cases, the amount of the active 5-hmC mark was also similar between ERWT and ERKO mice, except for a slight decrease in the #1.2 and an increase in the #1.3 ER BSs that paralleled their levels of H3K4me2. It could therefore be proposed that the #1.3 enhancer is in fact a counter-example gaining some chromatin functionality.

Interestingly, clusters 4, 8 and 9 include ER BSs located away from TSSs and could thus be defined as putative enhancers (**Fig. 6A**). However, we did not find evidence of any motif for a transcription factor specific to cluster 8 or 9 that could explain why changes in H3K4me2 enrichment occur in the latter and not the former (motif analysis provided within **Supplemental File 4**). We previously observed that ER BSs were highly enriched in HNF4 motifs (see **Table2** and **Supplemental Figure 6**), another nuclear receptor, crucial for liver functions (73). This led us to determine whether its presence may protect ER BSs from losing their chromatin functionality in ERKO livers. As previously performed for ER, we determined Hnf4 $\alpha$  cistrome with different *p*-values to allow comparison between the different conditions, using data from another study (54). As shown within **Fig. 8A** and illustrated within the heatmap in **Fig. 8B**, we found that up to almost 77% of ER BSs were actually overlapping with Hnf4  $\alpha$  BSs. Importantly, when this overlap was lower for ER BSs belonging to clusters 7 and 9 (**Fig. 8C**), which are changing their functionality/poised state in ERKO livers. Therefore, this tie in with our hypothesis of a protective role of Hnf4  $\alpha$  against the loss of H3K4me2 mark on lost ER BSs.

In summary, together these observations indicate that a loss of ER in the liver does not strongly impact the chromatin status of its BSs: only those with a reduced overlap with Hnf4 $\alpha$  binding seem to present a less stable H3K4me2-marked nucleosome at their center.

#### **A proportion of the mouse liver Foxa2 cistrome is ER-dependent**

Our genomic data are in favor of ER acting on chromatin regions whose activation is independent of ER-binding. This could reflect the possible actions of an ortholog of a pioneering factor such as human FOXA1 (15,19). Foxa proteins are expressed in mouse liver, including the related Foxa1 and Foxa2 (74,75), and these proteins have been found to serve as a scaffold for ER to regulate gene transcription in the liver and prevent hepatocarcinogenesis (20,21). Hnf4 $\alpha$  binding in mouse liver is also conditioned (at least on part of its sites) during development by Foxa2 (76,77). We therefore

sought to investigate the role of these proteins in the creation of an ER cistrome and mapped their binding sites by ChIP-seq using liver chromatin preparations from the same animals as those used for the ER ChIP-seq experiments. We first observed that the Foxa1 and Foxa2 cistromes were very similar, due to a cross-reaction of Foxa1 antibodies against the Foxa2 protein (data not shown). The Foxa1 cistrome was therefore not analyzed in the subsequent step. As previously, we determined the Foxa2 cistromes with different  $p$ -values. Whatever the significance level used, we observed that the Foxa2 cistrome was reduced in ERKO mice compared to ERWT mice (**Fig. 9A**), with 5,991 Foxa2 BSs determined at a  $10^{-4}$   $p$ -value for ERKO compared to 11,767 for ERWT mice. As depicted within **Fig. 9B**, depending upon the  $p$ -value, 12 to 30% of ER BSs were found to recruit Foxa2, corresponding to 6-12% of the entire Foxa2 cistrome. Up to almost 90% of the Foxa2 sites identified in ERKO mice were also determined as Foxa2-positive in wild-type animals. At a fixed  $p$ -value of  $10^{-4}$ , we identified 7,746 lost Foxa2 BSs (**Fig. 9C**). Importantly, only a sixth of these lost sites (688+491=1,179) were ER-positive (**Fig. 9C**). These data indicate that the loss of Foxa2 binding could be, at least in part, an indirect effect of ER depletion. The Foxa2 ChIP-seq signal was apparently lower in ERKO mice than in ERWT mice at conserved sites (see heatmap in **Fig. 9D** and mean values in **Fig. 9E**), indicating that Foxa2 binding events might also be less frequent in livers not expressing ER. However, although independent ChIP-qPCR experiments mostly recapitulated the expected results on gained and lost Foxa2 sites (**Supplemental Fig. 11, Fig. 9F**), a significantly reduced mobilization of this factor was observed for only 1 (#4.7) out of 10 tested conserved Foxa2 BSs (**Fig. 9F**). We hypothesize that the highly heterogeneous enrichments obtained for the different samples may have hindered the detection of possible differences. Importantly, although our microarray data indicated that Foxa2 mRNA expression was 10% lower in ERKO livers, this regulation was neither systematic nor significant as assessed by independent RT-qPCR and Western blot experiments (**Supplemental Fig. 3** and **Supplemental Fig. 12**).

#### **Variations in the H3K4me2 content of nucleosomes included in lost Foxa2 BSs**

To better comprehend the possible events occurring at Foxa2 BSs in ERKO vs. ERWT livers, we used our ERWT and ERKO H3K27ac and H3K4me2 ChIP-seq data to determine the relative genome-wide enrichment of Foxa2 BSs in these chromatin modifications that indicate active/poised enhancers.

As described previously for lost ER BSs, changes were observed only at Foxa2 BSs located within putative enhancers (data not shown). We therefore focused our analysis on BSs situated >5 kb from any annotated gene promoter and aligned the mean H3K4me2 and H3K27ac ChIP-seq signals to these sites (**Fig. 10A**). Data obtained indicate that there was a loss of the biphasic shape of enrichment in H3K4me2 in ERKO compared to ERWT mice at these lost Foxa2 BSs (seen enlarged view in **Fig. 10A**). In contrast, both the shape and level of enrichment of these sites in H3K27ac were unaffected (**Fig. 10A**). To evaluate a possible direct link between ER expression and these changes in chromatin modifications at Foxa2 BSs, we subdivided lost Foxa2 BSs into those which concomitantly recruited ER or those which did not (**Fig. 10B**). In contrast to their unchanged H3K27ac levels, we observed that the enrichment of both categories of sites in H3K4me2 was lower in ERKO livers compared to ERWT. Importantly, this was also associated with the disappearance of the biphasic shape of H3K4me2 enrichment (**Fig. 10B**), a biphasic-to-monophasic change that was observed neither at conserved Foxa2 BSs nor at novel ones (**Fig. 10A**). This demonstrated that the observed changes were not generated due to a bias of the normalization of the ChIP-seq signals but rather reflected a significant change in the enrichment of nucleosomes surrounding or centered on lost Foxa2 BSs in H3K4me2. Furthermore, such a change in shape was not observed at the BSs determined in mouse liver for other transcription factors such as Ctf, Ppara, Rxra, GR and Esrra (not shown).

Independent ChIP-qPCR experiments (data and statistics provided in **Supplemental Fig. 10**) following the enrichment of some Foxa2 BSs in H3K4me1 and H3K4me2 mostly recapitulated the conclusions obtained from genome-wide studies, *i.e.* that there is a reduction in the amount of methylated H3K4 in nucleosomes surrounding lost Foxa2 BSs in livers from ERKO mice (**Fig. 10C**). These effects were small, which may reflect the slight reduction observed in the amplitude of the mean profiles of the whole-genome data. Furthermore, due to the limited resolution of ChIP-qPCR experiments, the transition from a biphasic to monophasic distribution over a 1.5-2 kb window may have little or even no impact on the qPCR-mediated amplification of a DNA fragment located within a Foxa2 BS. Interestingly, we also observed a reduction in the acetylation of H3K27 on four of these sites, which was not expected from the whole-genome ChIP-seq data. MeDIP evaluation of the 5-mC amounts present within lost Foxa2 BSs also showed no variations between ERWT and ERKO livers

(**Supplemental Fig. 10; Fig. 10D**). Altogether, these data indicate that the Foxa2-positive enhancers which were lost in ERKO livers did not undergo complete chromatin closure. This conclusion is reinforced by the fact that only two of the 15 tested Foxa2 BSs (#4.6 and #1.2) had reduced amounts of 5-hmC in ERKO livers (**Fig. 10D**).

#### **Liver-specific transcription factor networks may secure FoxA2 cistrome**

In order to gain further insights into the mechanisms responsible for the loss of Foxa2 BSs in ERKO liver, we next examined whether particular transcription factors could either protect the conserved Foxa2 BSs from loss, or be responsible for the loss. Reassuringly, the most enriched motifs in each group were those recognized by Foxa2 and other members of the Forkhead family of TFs (**Table 4**, example Wordle picture is given in **Figure 11A** for lost FoxA2 BSs; full analysis is provided within **Supplemental File 3**). Besides Forkhead motifs, the sequences of the three Foxa2 BSs' category included similar sets of motifs for TF binding. The most frequently identified sequences were those recruiting CEBP, HNF4 $\alpha$  and other NRs such as RXR, RAR, NR1D1/D2, or the tumor suppressor NKX3-1. Importantly, CEBPA/B and HNF4 $\alpha$  are known "liver-enriched" transcription factors (78-80). When examined more precisely, 38 or 68 motifs were specifically identified within lost or conserved Foxa2BSs respectively (**Supplemental Fig.13**). However, the different sets of TFs binding to these specific motifs do not create networks that can be associated with specific functions, as evaluated by their annotations through STRING (81; see **Supplemental Fig.13**) Furthermore, the expression levels of the transcription factors associated with these DNA sequences were not significantly affected by the inactivation of the *Esr1* gene (**Supplemental Fig. 13**).

Finally, we compared our different categories of Foxa2 BSs to the available cistromes of other TF determined by others in mouse livers. Those included Cebp $\alpha$  and Cebp $\beta$ , Hnf4 $\alpha$ , other nuclear receptors, repressive co-regulators (Hdac and Ncor1) and Ctf. We also included Nkx3-1 in our analyses since its motif was the most enriched in all Foxa2 BSs categories following FKH motifs. Furthermore, NKX3-1 was demonstrated to act as an inhibitor of ER activity in human cancer cells (82). Note however that the only available cistrome of this factor in mouse was determined in prostate. We also integrated a Foxa1 cistrome, although it may not be totally specific and include FoxA2 BSs. Strikingly, we observed that the overlaps of the conserved Foxa2 BSs with the cistromes of Foxa1,

ER, Hnf4 $\alpha$ , Nkx3-1, Cebp $\alpha$ , Cebp $\beta$  and Rxr $\alpha$  were significantly higher as compared to what was observed for lost or gained Foxa2 BSs (**Fig. 11B**). This indicates that the binding of (at least) one of these other TFs -excluding ER of course- to genomic regions may help to preserve Foxa2 binding at these sequences. Interestingly, Hnf4 $\alpha$ , Cebp $\alpha$  and Cebp $\beta$  were also found to be more often recruited on sites conserving their H3K4me2 or H3K27ac levels rather than on genomic regions with reduced or gained enrichment in these chromatin marks in ERKO livers (**Supplemental Fig. 14**). This suggests that this combination of factors may generally prevent changes of chromatin functionality to occur on the sites they engage in ERKO livers.

## Discussion

The objectives of this study were dual: *i*) to identify mechanisms of actions of hepatic ER *in vivo* and in particular to test whether it can exert some influence in the absence of its ligand, and *ii*) to characterize short-term changes in liver response to estrogens following acute E2 administration that could explain how E2 could have opposite influences in liver.

Indeed, a number of studies have demonstrated in rodents that E2 has protective roles against metabolic abnormalities: ovariectomy, whole body ER knock-out (ERKO) and aromatase KO, are all associated with increased body weight, impaired glucose tolerance, insulin resistance (IR) and liver steatosis (23,24,83). In contrast, the administration of estrogens by the oral route prescribed for contraception or for hormonal replacement therapy at menopause is associated with an increased risk of venous thrombosis and pulmonary embolism, presumably due to the impact of E2 on liver coagulation factor expression or activity. Here, we characterized in mouse liver sets of E2- and ER-dependent genes which were associated with lipogenesis, but none with coagulation. Accordingly, the genes predicted to be controlled by enhancer regions losing or gaining the active chromatin marks H3K4me2 and H3K27ac in ERKO livers were associated with liver-specific functions (**Supplemental Fig. 8**). These observations tied in with the crucial role of ER in E2-mediated prevention of liver steatosis in mice fed with high fat diet. They also highlight species differences in the regulation of coagulation factors by E2 between human and mouse (84). We observed that 48 of the 110 E2-

regulated genes identified here were also regulated following chronic estrogen treatment for three days (36). This number drastically decreased to only two common genes after a two week treatment (37) or even one when comparing our list with a dataset generated from isolated liver cells (33). This latter observation could be explained by the adaptation of the liver cell transcriptome following cell culture, a transcriptome that also depends on the culture conditions (85,86). These differences between the estrogen-sensitive transcriptomes following chronic or acute treatment of hormones indicate that each mode of administration or time of treatment has a differential physiological impact.

Using conditions of short-term E2 administration and freshly-dissected liver, we detected ER binding to less than 4,000 genomic regions by ChIP-seq. This contrasts with the much larger ER cistromes determined in cultured human mammary cell lines such as MCF-7 cells (11,12). Interestingly, although we used chromatin prepared from livers treated for different times, our data are in agreement with some other studies that have also found limited ER cistromes in liver (43,58). Furthermore, it is tempting to speculate that this limited number of ER BSs could be the cause of the lower number of E2-regulated genes identified here in liver as compared to classical *in vitro* model such as cultured MCF-7 cells (up to 1,500 regulated genes; see 34 and ref 87). A large set of ER BSs was also determined in isolated mouse liver cells (33), which presented 3-fold more E2-sensitive genes than determined here following acute E2 treatment of liver. Importantly, although ~2-fold less numerous, 60% of the E2-bound ER BSs determined here were in common with those determined in (33). As discussed above, the discrepancy in the number of ER BSs could also be a direct consequence of the conditions of E2-treatment or liver cell differentiation. These conditions might, for instance, influence the expression of chaperone proteins such as p23, whose over-expression in MCF-7 breast cancer cells is reported to enhance the number of ER BSs (88). However, we determined that 72% of the 5,526 ER BSs identified by our pipeline using a ChIP-seq dataset generated from the liver of non-ovariectomized females (20) were in common with the different ER cistromes determined in E2-treated livers from ovariectomized females (**Supplemental Fig. 4**). This suggests that the ER cistrome may present some robustness in liver, contrasting with an intrinsically more versatile hepatic transcriptome generated by (i) a cellular heterogeneity; and (ii) a high number of individual-specific regulatory influences (metabolic/detoxification...). Importantly, as is the case for all other reported



ER cistromes in liver, a significant fraction of the ER BSs identified here were found to be located in relatively close proximity to E2 regulated genes (7 to 12%), compared to MCF-7 data (2%). A general consequence of the organization of the genome within the nucleus is the existence of chromatin loops (89) that link distant regulatory elements such as ER BSs to their target genes (90) within large (1 Mb) topologically associating chromatin domains (TADs) (91). Although long-range interactions between enhancers and gene promoters do of course exist in mouse liver (92,93), our data point to the hypothesis that their multiplicity and possible functional redundancy (34,94) might be curtailed *in vivo* for E2-transcriptional responses within this tissue. This could also be true in the uterus, in which almost 16% of the ER BSs were located <3 kb from gene TSSs (Supplemental Fig. 7) (41). Additionally, enhanced stability of the loops between enhancers and TSSs may also increase the number of detected binding events at promoters, which would have to be considered as phantom imprints of this stable chromatin organization. However, the observed enrichment of these proximal ER BSs in motifs that are able to directly recruit ER (EREs, AP1 or Sp1) partly excludes this hypothesis.

We have also determined that ER could be detected at approximately 850 ER BSs in untreated livers from ovariectomized female mice, 40% of them also being engaged by ER in the presence of E2. However, the existence and functionality of the remaining 476 placebo-specific ER BSs remains unclear. These placebo-specific sites were not found enriched at the proximity of genes whose expression was repressed by E2, and less than 2% of them were located closer than 10 kb from the TSS of any annotated gene (data not shown). Furthermore, independent ChIP assays performed with an antibody directed against the N-terminal region of ER were able to confirm an ER commitment at only 5 of the 19 randomly chosen regions falling into the placebo-specific condition. This could reflect a problem of specificity of the antibody directed against the C-terminal region of the protein, since it was able to purify 40 genomic regions supposedly binding to ER in ERKO livers. Alternatively, the epitopes targeted by the anti N-terminal antibody may be less accessible than those recognized by the C-terminal antibody, although the recent structure of a DNA-bound ER complexed with cofactors would suggest the opposite (95). Finally, we can also postulate that the placebo-specific ER BSs may specifically recruit the ER $\alpha$  46 or ER $\alpha$  36 isoforms of ER which are devoid of



its N-terminal region and are known to be expressed in mouse liver (96-98). Investigating this hypothesis will require the whole-genome cartography of the binding events of these isoforms to be established using specific antibodies combined with the generation of corresponding mouse models expressing only one of the three ER isoforms.

Comparing the transcriptomes and the distribution of H3K4me2 and H3K27ac chromatin marks within the genome of ERWT and ERKO livers raised several novel insights into the roles of ER in mouse liver. First, from a chromatin point of view, we observed that the enrichment of genes promoters in active marks globally paralleled their differential expression in ERKO as compared to ERWT livers. This correlation was slightly more important for up-regulated than down-regulated genes, suggesting that chromatin changes accompanying genes with higher transcriptional activity are more drastic than those observed for genes with reduced activity. Second, among the 129 genes differently expressed in the livers of ERKO vs. ERWT mice, only 10 were also regulated by E2 in ERWT. On the one hand, this observation could reflect the fact that the remaining 119 genes are indirectly regulated by ER, *i.e.* that one or more proteins or RNAs regulated by ER and/or E2 is required for the correct expression of these genes. Note that this faulty regulatory component could be expressed in the liver itself but since we used whole body ER knock-out (KO) mice it could also be expressed in other organs and indirectly influence the signalling cascades in the liver. This hypothesis is supported by the fact that these genes do not have any ER BSs in their vicinity. On the other hand, this observation also indicates that ER is not absolutely required for the basal expression of the majority of the E2-sensitive genes in the liver. This demonstrates *in vivo* that ER has to be considered as a regulator of transcription rather than a required factor for the transcription of these genes. Such a conclusion can also be drawn from our MeDIP-qPCR and H3K4me2/H3K27ac ChIP-seq data, which demonstrated that ER is not required *per se* for the establishment and/or maintenance of chromatin modifications at the majority of its binding sites. Moreover, we found that ER BSs with reduced chromatin functionality in ERKO are less frequently associated with the liver master regulator Hnf4α (76-80).

These observations pointing at a secondary role of ER for the functionality of liver chromatin are also perfectly compatible with the notion that ER and other TFs act subsequent to the required

preliminary actions of pioneering factors such as FOXA proteins, or other partners such as GATA, C/EBP, etc (15,99,100) which determine the functionalization and accessibility of chromatin. However, contrasting with this pioneering view, we found that Foxa2 mobilization was affected in ERKO livers, even at ER-negative Foxa2 BSs identified in ERWT mice. Importantly, independent RT-qPCR or Western blot experiments did not consistently reproduce the 10% drop in Foxa2 expression in ERKO livers detected by our microarray data. It is possible that the heterogeneity of the liver transcriptome and its dependence on the mouse diet may have hindered the detection of variations in Foxa2 expression. To get further information on a putative ER-mediated regulation of Foxa2, we hypothesized that if ER was controlling the expression of Foxa2 there might be genes regulated in the same way in ERKO and Foxa2KO mice. Comparison of our dataset with those available for a liver-specific double Foxa1/Foxa2 KO (22) revealed that 21 of the 721 Foxa-dependent mRNAs also had reduced expression in ERKO mice (data not shown). These genes exhibited no annotation towards a specific pathway or biological process. Although we cannot formerly exclude the possibility that Foxa2 expression may be influenced by the loss of ER expression, so far there is no clear evidence of a particular functional consequence of this putative direct relationship.

Nevertheless, a 10% drop in Foxa2 expression may not be sufficient to explain a 50% loss in Foxa2 BSs. An in depth motif analysis associated with a comparison of Foxa2 BSs with the available cistromes of other TFs allowed us to provide an hypothetical model in which the binding of a network of other TFs on shared BSs may protect these sites from totally losing FoxA2 engagement and chromatin functionality. These factors are Hnf4 $\alpha$ , Nkx3-1, Cebp $\alpha$ , Cebp $\beta$  and Rxra and possibly Foxa1. Although we cannot ascertain the perfect specificity of our Foxa1 cistrome because of antibodies cross-reactivity with Foxa2, it may be interesting to note that 188 putative “ERKO-specific” Foxa1 sites were determined as lost Foxa2 BSs (data not shown). Interestingly, we also determined that regions that totally lost their central H3K4me2-enriched nucleosome were including DNA recognition motifs for Tead and Tcfap2 factors (**Supplementary Fig. 14**). AP2 is a pioneer factor, and may exert here a direct function in controlling chromatin opening. Tead factors, and in particular Tead 2 are involved in Foxa2/Hnf4 $\alpha$  enhancer selection during hepatocyte differentiation (76). These two factors may therefore be integrated into the network of TFs that protect against chromatin

changes in ERKO livers. However, whether these factors direct the mobilization of chromatin modifiers that specifically prevent FoxA2 disengagement remains to be directly evaluated. Candidate modifiers could be proposed from our H3K4me2 ChIP-seq data showing a shift from a biphasic to a perfectly centered monophasic shape on some ER BSs and lost FoxA2 BSs. Two mechanisms could explain these observations: either the central nucleosome is preferentially modified by an H3K4 methylase in ERKO livers (or the adjacent ones are not modified at all), or the absence of ER or FoxA2 directly or indirectly affects nucleosome positioning. In MCF-7 cells, ER genomic activity was shown to depend on the H3K methylases SMYD3, SETD1A, MLL1 or MLL2 (10,101-104), and even on its direct methylation by SMYD2 (105,106). However, mRNA encoding the orthologs of these proteins did not exhibit significant changes in ERKO relative to ERWT livers (not shown). The same was also true concerning the expression of histone chaperones involved in nucleosome positioning and dynamics, such as Spt16h and Ssrp1, components of FACT (107), or Spt6h and nucleolin (108).

In conclusion, we have demonstrated here that the actions of ER and the acute administration of E2 in mouse liver *in vivo* have particular characteristics. Another important outcome of this study is the fact that ER is not absolutely required for the basal expression of the majority of the E2-sensitive genes in the liver and that it appears to be dispensable for the establishment and/or maintenance of chromatin modifications at the majority of its binding sites, where other TFs such as Hn4α may preserve functional competence. In contrast, ER was found required for the binding of the Foxa2 factor. Taken together, together, our results indicate that the loss of ER expression in livers from ERKO mice affects the distribution of H3K4me2-enriched nucleosomes around both ER BSs and Foxa2 BSs. The underlying mechanisms still remain to be understood, although they are likely independent of the transcriptional regulation of chromatin actors. Importantly, besides its genomic influences, ER exerts membrane- and/or cytoplasmic-based actions on intracellular kinase transduction pathways (109). Hence, it would be interesting to test whether ER could regulate the activity of Foxa2 or H3K4 methylases at the post-translational level in liver using specific mouse models expressing ER forms devoid of either nuclear- (110,111) or membrane-based regulatory abilities (112,113).

713

714 **Acknowledgements**

715 The staff of the animal facilities of the “Plateforme d’experimentation fonctionnelle” (A.  
716 Desquesnes) in Toulouse, M. Buscato and F. Boudou, are acknowledged for skillful technical  
717 assistance. We greatly acknowledge S. Vicaire, S. Le Gras, M. Philipps and B. Jost for their  
718 indispensable help and work on generating the HTS data at the IGBMC Microarray and Sequencing  
719 platform at Illkirch. We also thank Y. Lippi and P. Martin for the excellent contribution to microarray  
720 analysis carried out at the GeT-TRIX Genopole Toulouse facility. Work performed at the UMR  
721 CNRS 6290 was supported by the “Centre National de la Recherche Scientifique” (CNRS), the  
722 University of Rennes I, and benefited from grants from the “Association pour la Recherche contre le  
723 Cancer” (ARC), the “Ligue Contre le Cancer” (Equipe Labellisée Ligue 2009), the “Région Bretagne”  
724 [CREATE #4793] and the “Agence Nationale pour la Recherche” [ANR-09-BLAN-0268-01].  
725 Support for the work carried out at INSERM U1085 was obtained from the “Institut national de la  
726 santé et de la recherche médicale” (INSERM), the University of Rennes I, and the “Ligue Contre le  
727 Cancer”. The work at the INSERM unit U1048 was supported by the INSERM, University of  
728 Toulouse III, Faculty of Medecine Toulouse-Rangueil, “Fondation de France”, “Conseil Régional  
729 Midi-Pyrénées” and “Fondation pour la Recherche Médicale” (FRM). Sequencing performed by the  
730 IGBMC Microarray and Sequencing platform was supported by the FG National Infrastructure,  
731 funded as part of the "Investissements d'Avenir" program managed by the “Agence Nationale pour la  
732 Recherche” [ANR-10-INBS-0009].

733

## References

1. **Couse JF, Korach KS.** Estrogen receptor null mice: what have we learned and where will they lead us? *Endocr Rev.* 1999;20:358-417.
2. **McEwan IJ.** Nuclear receptors: one big family. *Methods Mol Biol.* 1999;505:3-18.
3. **Lenfant F, Trémollières F, Gourdy P, Arnal JF.** Timing of the vascular actions of estrogens in experimental and human studies: why protective early, and not when delayed? *Maturitas.* 2011;68:165-173.
4. **Carroll JS, Brown M.** Estrogen receptor target gene: an evolving concept. *Mol Endocrinol.* 2006;20:1707-1714.
5. **Eeckhoute J, Métivier R, Salbert G.** Defining specificity of transcription factor regulatory activities. *J Cell Sci.* 2009;122:4027-4034.
6. **Magnani L, Eeckhoute J, Lupien M.** Pioneer factors: directing transcriptional regulators within the chromatin environment. *Trends Genet.* 2011;27:465-474.
7. **Shang Y, Hu X, DiRenzo J, Lazar MA, Brown M.** Cofactor dynamics and sufficiency in estrogen receptor-regulated transcription. *Cell.* 2000;103:843-852.
8. **Métivier R, Penot G, Hübner MR, Reid G, Brand H, Kos M, Gannon F.** Estrogen receptor- $\alpha$  directs ordered, cyclical, and combinatorial recruitment of cofactors on a natural target promoter. *Cell.* 2003;115:751-763.
9. **Zwart W, Theodorou V, Kok M, Canisius S, Linn S, Carroll JS.** Oestrogen receptor-cofactor-chromatin specificity in the transcriptional regulation of breast cancer. *EMBO J.* 2011;30:4764-4776.
10. **Wong Jeong K, Chodankar R, Purcell DJ, Bittencourt D, Stallcup MR.** Gene-specific patterns of coregulator requirements by estrogen receptor- $\alpha$  in breast cancer cells. *Mol Endocrinol.* 2012;26:955-966.
11. **Carroll JS, Meyer CA, Song J, Li W, Geistlinger TR, Eeckhoute J, Brodsky AS, Keeton EK, Fertuck KC, Hall GF, Wang Q, Bekiranov S, Sementchenko V, Fox EA, Silver PA,**

- Gingeras TR, Liu XS, Brown M.** Genome-wide analysis of estrogen receptor binding sites. *Nat Genet.* 2006;38:1289-1297.
12. **Welboren WJ, Sweep FC, Span PN, Stunnenberg HG.** Genomic actions of estrogen receptor alpha: what are the targets and how are they regulated? *Endocr Relat Cancer.* 2009;16:1073-1089.
13. **Hah N, Murakami S, Nagari A, Danko CG, Kraus WL.** Enhancer transcripts mark active estrogen receptor binding sites. *Genome Res.* 2013;23:1210-1223.
14. **Li W, Notani D, Ma Q, Tanasa B, Nunez E, Chen AY, Merkurjev D, Zhang J, Ohgi K, Song X, Oh S, Kim HS, Glass CK, Rosenfeld MG.** Functional roles of enhancer RNAs for oestrogen-dependent transcriptional activation. *Nature.* 2013;498:516-520.
15. **Zaret KS, Carroll JS.** Pioneer transcription factors: establishing competence for gene expression. *Genes Dev.* 2011;25:2227-2241.
16. **Cirillo LA, Zaret KS.** An early developmental transcription factor complex that is more stable on nucleosome core particles than on free DNA. *Mol Cell.* 1999;4:961-969.
17. **Cirillo LA, Lin FR, Cuesta I, Friedman D, Jarnik M, Zaret KS.** Opening of compacted chromatin by early developmental transcription factors HNF3 (FoxA) and GATA-4. *Mol Cell.* 2002;9:279-289.
18. **Soufi A, Garcia MF, Jaroszewicz A, Osman N, Pellegrini M, Zaret KS.** Pioneer transcription factors target partial DNA motifs on nucleosomes to initiate reprogramming. *Cell.* 2015;161:555-568.
19. **Hurtado A, Holmes KA, Ross-Innes CS, Schmidt D, Carroll JS.** FOXA1 is a key determinant of estrogen receptor function and endocrine response. *Nat Genet.* 2011;43:27-33.
20. **Li Z, Tuteja G, Schug J, Kaestner KH.** Foxa1 and Foxa2 are essential for sexual dimorphism in liver cancer. *Cell.* 2012;148:72-83.
21. **Zhao Y, Li Z.** Interplay of estrogen receptors and FOXA factors in the liver cancer. *Mol Cell Endocrinol.* 2015. doi: 10.1016/j.mce.2015.01.043. [Epub ahead of print].
22. **Li Z, Schug J, Tuteja G, White P, Kaestner KH.** The nucleosome map of the mammalian liver. 2011; *Nat Struct Mol Biol*;18:742-746.

- 788 23. **Zhu L, Brown WC, Cai Q, Krust A, Chambon P, McGuinness OP, Stafford JM.** Estrogen  
789 treatment after ovariectomy protects against fatty liver and may improve pathway-selective  
790 insulin resistance. *Diabetes*. 2013;62:424-434.
- 791 24. **Han SI, Komatsu Y, Murayama A, Steffensen KR, Nakagawa Y, Nakajima Y, Suzuki M,**  
792 **Oie S, Parini P, Vedin LL, Kishimoto H, Shimano H, Gustafsson JÅ, Yanagisawa J.**  
793 Estrogen receptor ligands ameliorate fatty liver through a nonclassical estrogen receptor/Liver X  
794 receptor pathway in mice. *Hepatology*. 2014;59:1791-1802.
- 795 25. **Tchaikovski SN, Rosing J.** Mechanisms of estrogen-induced venous thromboembolism. *Thromb*  
796 *Res*. 2010;126: 5-11.
- 797 26. **Canonico M, Oger E, Plu-Bureau G, Conard J, Meyer G, Lévesque H, Trillot N, Barrellier**  
798 **MT, Wahl D, Emmerich J, Scarabin PY, Estrogen and Thromboembolism Risk (ESTHER)**  
799 **Study Group.** Hormone therapy and venous thromboembolism among postmenopausal women:  
800 impact of the route of estrogen administration and progestogens: the ESTHER study. *Circulation*.  
801 2007;115:840-845.
- 802 27. **van Nas A, Guhathakurta D, Wang SS, Yehya N, Horvath S, Zhang B, Ingram-Drake L,**  
803 **Chaudhuri G, Schadt EE, Drake TA, Arnold AP, Lusi AJ.** Elucidating the role of gonadal  
804 hormones in sexually dimorphic gene coexpression networks. *Endocrinology*. 2009;150:1235-  
805 1249.
- 806 28. **Pedram A, Razandi M, O'Mahony F, Harvey H, Harvey BJ, Levin ER.** Estrogen reduces  
807 lipid content in the liver exclusively from membrane receptor signaling. *Sci Signal*. 2013;6:ra36.
- 808 29. **Matic M, Bryzgalova G, Gao H, Antonson P, Humire P, Omoto Y, Portwood N, Pramfalk**  
809 **C, Efendic S, Berggren PO, Gustafsson JÅ, Dahlman-Wright K.** Estrogen signalling and the  
810 metabolic syndrome: targeting the hepatic estrogen receptor alpha action. *PLoS One*.  
811 2013;8:e57458.
- 812 30. **Dupont S, Krust A, Gansmuller A, Dierich A, Chambon P, Mark M.** Effect of single and  
813 compound knockouts of estrogen receptors alpha (ERalpha) and beta (ERbeta) on mouse  
814 reproductive phenotypes. *Development*. 2000;127:4277-4291.



31. **Zhang B, Kirov S, Snoddy J.** WebGestalt: an integrated system for exploring gene sets in various biological contexts. *Nucleic Acids Res.* 2005;33:W741-748.
32. **Barrett T, Troup DB, Wilhite SE, Ledoux P, Rudnev D, Evangelista C, Kim IF, Soboleva A, Tomashevsky M, Marshall KA, Phillippy KH, Sherman PM, Muerdtter RN, Edgar R.** NCBI GEO: archive for high-throughput functional genomic data. *Nucleic Acids Res.* 2009;37:D885-890.
33. **Gordon FK, Vallaster CS, Westerling T, Iyer LK, Brown M, Schnitzler GR.** Research Resource: Aorta- and Liver-Specific ER $\alpha$ -Binding Patterns and Gene Regulation by Estrogen. *Mol Endocrinol.* 2014;28:1337-1351.
34. **Quintin J, Le Péron C, Palierne G, Bizot M, Cunha S, Sérandour AA, Avner S, Henry C, Percevault F, Belaud-Rotureau MA, Huet S, Watrin E, Eeckhoute J, Legagneux V, Salbert G, Métivier R.** Dynamic estrogen receptor interactomes control estrogen-responsive trefoil Factor (TFF) locus cell-specific activities. *Mol Cell Biol.* 2014;34:2418-2436.
35. **Sérandour AA, Avner S, Oger F, Bizot M, Percevault F, Lucchetti-Miganeh C, Palierne G, Gheeraert C, Barloy-Hubler F, Le Péron C, Madigou T, Durand E, Froguel P, Staels B, Lefebvre P, Métivier R, Eeckhoute J, Salbert G.** Dynamic hydroxymethylation of deoxyribonucleic acid marks differentiation-associated enhancers. *Nucleic Acids Res.* 2012;40:8255-8265.
36. **Langmead B, Trapnell C, Pop M, Salzberg SL.** Ultrafast and memory-efficient alignment of short DNA sequences to the human genome. *Genome Biol.* 2009;10:R25.
37. **Li H, Handsaker B, Wysoker A, Fennell T, Ruan J, Homer N, Marth G, Abecasis G, Durbin R, 1000 Genome Project Data Processing Subgroup.** The Sequence Alignment/Map format and SAMtools. *Bioinformatics.* 2009;25:2078-2079.
38. **Zhang Y, Liu T, Meyer CA, Eeckhoute J, Johnson DS, Bernstein BE, Nusbaum C, Myers RM, Brown M, Li W, Liu XS.** Model-based analysis of ChIP-Seq (MACS). *Genome Biol.* 2008;9:R137.



- 841 39. **Liu T, Ortiz A, Taing L, Meyer CA, Lee B, Zhang Y, Shin H, Wong SS, Ma J, LeiY, Pape**  
842 **UJ, Poidinger M, Chen Y, Yeung K, Brown M, Turpaz Y, Liu XS.** Cistrome: an integrative  
843 platform for transcriptional regulation studies. *Genome Biol.* 2011;12:R83.
- 844 40. **Kolesnikov N, Hastings E, Keays M, Melnichuk O, Tang YA, Williams E, Dylag M,**  
845 **Kurbatova N, Brandizi M, Burdett T, Megy K, Pilicheva E, Rustici G, Tikhonov A,**  
846 **Parkinson H, Petryszak R, Sarkans U, Brazma A.** ArrayExpress update--simplifying data  
847 submissions. *Nucleic Acids Res.* 2015;43: D1113-1116.
- 848 41. **Hewitt SC, Li L, Grimm SA, Chen Y, Liu L, Li Y, Bushel PR, Fargo D, Korach KS.**  
849 Research resource: whole-genome estrogen receptor  $\alpha$  binding in mouse uterine tissue revealed  
850 by ChIP-seq. *Mol Endocrinol.* 2012;26:887-898.
- 851 42. **Schmidt D, Schwalie PC, Ross-Innes CS, Hurtado A, Brown GD, Carroll JS, Flicek P,**  
852 **Odom DT.** A CTCF-independent role for cohesin in tissue-specific transcription. *Genome Res.*  
853 2010;20:578-88.
- 854 43. **Gao H, Fält S, Sandelin A, Gustafsson JA, Dahlman-Wright K.** Genome-wide identification  
855 of estrogen receptor alpha-binding sites in mouse liver. *Mol Endocrinol.* 2008;22:10-22.
- 856 44. **Qin B, Zhou M, Ge Y, Taing L, Liu T, Wang Q, Wang S, Chen J, Shen L, Duan X, Hu S, Li**  
857 **W, Long H, Zhang Y, Liu XS.** CistromeMap: a knowledgebase and web server for ChIP-Seq  
858 and DNase-Seq studies in mouse and human. *Bioinformatics.* 2012;28:1411-1412.
- 859 45. **Sun H, Qin B, Liu T, Wang Q, Liu J, Wang J, Lin X, Yang Y, Taing L, Rao PK, Brown M,**  
860 **Zhang Y, Long HW, Liu XS.** CistromeFinder for ChIP-seq and DNase-seq data reuse.  
861 *Bioinformatics.* 2013;29:1352-1354.
- 862 46. **MacIsaac KD, Lo KA, Gordon W, Motola S, Mazor T, Fraenkel E.** A quantitative model of  
863 transcriptional regulation reveals the influence of binding location on expression. *PLoS Comput*  
864 *Biol.* 2010;6:e1000773.
- 865 47. **Schmidt D, Wilson MD, Ballester B, Schwalie PC, Brown GD, Marshall A, Kutter C, Watt**  
866 **S, Martinez-Jimenez CP, Mackay S, Talianidis I, Flicek P, Odom DT.** Five-vertebrate ChIP-  
867 seq reveals the evolutionary dynamics of transcription factor binding. *Science.* 2010;328:1036-40.

- 868 48. **Boergesen M, Pedersen TÅ, Gross B, van Heeringen SJ, Hagenbeek D, Bindesbøll C, Caron**  
869 **S, Lalloyer F, Steffensen KR, Nebb HI, Gustafsson JÅ, Stunnenberg HG, Staels B,**  
870 **Mandrup S.** Genome-wide profiling of liver X receptor, retinoid X receptor, and peroxisome  
871 proliferator-activated receptor  $\alpha$  in mouse liver reveals extensive sharing of binding sites. *Mol*  
872 *Cell Biol.* 2012;32:852-67.
- 873 49. **Grøntved L, John S, Baek S, Liu Y, Buckley JR, Vinson C, Aguilera G, Hager GL.** C/EBP  
874 maintains chromatin accessibility in liver and facilitates glucocorticoid receptor recruitment to  
875 steroid response elements. *EMBO J.* 2013;32:1568-83.
- 876 50. **Chaveroux C, Eichner LJ, Dufour CR, Shatnawi A, Khoutorsky A, Bourque G, Sonenberg**  
877 **N, Giguère V.** Molecular and genetic crosstalks between mTOR and  $ERR\alpha$  are key determinants  
878 of rapamycin-induced nonalcoholic fatty liver. *Cell Metab.* 2013;17:586-98.
- 879 51. **Bugge A, Feng D, Everett LJ, Briggs ER, Mullican SE, Wang F, Jager J, Lazar MA.** Rev-  
880  $erb\alpha$  and Rev- $erb\beta$  coordinately protect the circadian clock and normal metabolic function.  
881 *Genes Dev.* 2012;26:657-67.
- 882 52. **Cho H, Zhao X, Hatori M, Yu RT, Barish GD, Lam MT, Chong LW, DiTacchio L, Atkins**  
883 **AR, Glass CK, Liddle C, Auwerx J, Downes M, Panda S, Evans RM.** Regulation of circadian  
884 behaviour and metabolism by REV-ERB- $\alpha$  and REV-ERB- $\beta$ . *Nature.* 2012;485:123-7.
- 885 53. **Shen Y, Yue F, McCleary DF, Ye Z, Edsall L, Kuan S, Wagner U, Dixon J, Lee L,**  
886 **Lobanenkov VV, Ren B.** A map of the cis-regulatory sequences in the mouse genome. *Nature.*  
887 2012;488:116-20.
- 888 54. **Alpern D, Langer D, Ballester B, Le Gras S, Romier C, Mengus G, Davidson I.** TAF4, a  
889 subunit of transcription factor II D, directs promoter occupancy of nuclear receptor HNF4A  
890 during post-natal hepatocyte differentiation. *Elife.* 2014;3:e03613.
- 891 55. **Anderson PD, McKissic SA, Logan M, Roh M, Franco OE, Wang J, Doubinskaia I, van der**  
892 **Meer R, Hayward SW, Eischen CM, Eltoum IE, Abdulkadir SA.** Nkx3.1 and Myc  
893 crossregulate shared target genes in mouse and human prostate tumorigenesis. *J Clin Invest.*  
894 2012;122:1907-19.

- 895 56. **Untergasser A, Cutcutache I, Koressaar T, Ye J, Faircloth BC, Remm M, Rozen SG.**  
 896 Primer3--new capabilities and interfaces. *Nucleic Acids Res.* 2012;40:e115.
- 897 57. **Saeed AI, Bhagabati NK, Braisted JC, Liang W, Sharov V, Howe EA, Li J, Thiagarajan M,**  
 898 **White JA, Quackenbush J.** TM4 microarray software suite. *Methods Enzymol.* 2006;411:134-  
 899 193.
- 900 58. **Villa A, Della Torre S, Stell A, Cook J, Brown M, Maggi A.** Tetradian oscillation of estrogen  
 901 receptor  $\alpha$  is necessary to prevent liver lipid deposition. *Proc Natl Acad Sci USA.*  
 902 2012;109:11806-11811.
- 903 59. **Joseph R, Orlov YL, Huss M, Sun W, Kong SL, Ukil L, Pan YF, Li G, Lim M, Thomsen JS,**  
 904 **Ruan Y, Clarke ND, Prabhakar S, Cheung E, Liu ET.** Integrative model of genomic factors  
 905 for determining binding site selection by estrogen receptor- $\alpha$ . *Mol Syst Biol.* 2010;6,:456.
- 906 60. **Ross-Innes CS, Stark R, Teschendorff AE, Holmes KA, Ali HR, Dunning MJ, Brown GD,**  
 907 **Gojis O, Ellis IO, Green AR, Ali S, Chin SF, Palmieri C, Caldas C, Carroll JS.** Differential  
 908 oestrogen receptor binding is associated with clinical outcome in breast cancer. *Nature.*  
 909 2012;481:389-393.
- 910 61. **Tang B, Hsu HK, Hsu PY, Bonneville R, Chen SS, Huang TH, Jin VX.** Hierarchical  
 911 modularity in ER $\alpha$  transcriptional network is associated with distinct functions and implicates  
 912 clinical outcomes. *Sci Rep.* 2012;2:875.
- 913 62. **Ovaska K, Matarese F, Grote K, Charapitsa I, Cervera A, Liu C, Reid G, Seifert M,**  
 914 **Stunnenberg HG, Hautaniemi S.** Integrative analysis of deep sequencing data identifies  
 915 estrogen receptor early response genes and links ATAD3B to poor survival in breast cancer.  
 916 *PLoS Comput Biol.* 2013;9:e1003100.
- 917 63. **McLean CY, Bristor D, Hiller M, Clarke SL, Schaar BT, Lowe CB, Wenger AM, Bejerano**  
 918 **G.** GREAT improves functional interpretation of cis-regulatory regions. *Nat Biotechnol.*  
 919 2010;28:495-501.
- 920 64. **Creyghton MP, Cheng AW, Welstead GG, Kooistra T, Carey BW, Steine EJ, Hanna J,**  
 921 **Lodato MA, Frampton GM, Sharp PA, Boyer LA, Young RA, Jaenisch R.** Histone H3K27ac

- 922 separates active from poised enhancers and predicts developmental state. *Proc Natl Acad Sci*  
 923 *USA*. 2010;107:21931-21936.
- 924 65. **Calo E, Wysocka J.** Modification of enhancer chromatin: what, how, and why? *Mol Cell*.  
 925 2013;49:825-837.
- 926 66. **Wang Y, Li X, Hu H.** H3K4me2 reliably defines transcription factor binding regions in different  
 927 cells. *Genomics*. 2014;103:222-228.
- 928 67. **Lister R, Pelizzola M, Downen RH, Hawkins RD, Hon G, Tonti-Filippini J, Nery JR, Lee L,**  
 929 **Ye Z, Ngo QM, Edsall L, Antosiewicz-Bourget J, Stewart R, Ruotti V, Millar AH, Thomson**  
 930 **JA, Ren B, Ecker JR.** Human DNA methylomes at base resolution show widespread  
 931 epigenomic differences. *Nature*. 2009;462:315-322.
- 932 68. **Song CX, Szulwach KE, Fu Y, Dai Q, Yi C, Li X, Li Y, Chen CH, Zhang W, Jian X, Wang**  
 933 **J, Zhang L, Looney TJ, Zhang B, Godley LA, Hicks LM, Lahn BT, Jin P, He C.** Selective  
 934 chemical labeling reveals the genome-wide distribution of 5-hydroxymethylcytosine. *Nat*  
 935 *Biotechnol*. 2011;29:68-72.
- 936 69. **Hoffman BG, Robertson G, Zavaglia B, Beach M, Cullum R, Lee S, Soukhatcheva G, Li L,**  
 937 **Wederell ED, Thiessen N, Bilenky M, Cezard T, Tam A, Kamoh B, Birol I, Dai D, Zhao Y,**  
 938 **Hirst M, Verchere CB, Helgason CD, Marra MA, Jones SJ, Hoodless PA.** Locus co-  
 939 occupancy, nucleosome positioning, and H3K4me1 regulate the functionality of FOXA2-,  
 940 HNF4A-, and PDX1-bound loci in islets and liver. *Genome Res*. 2010;20:1037-1051.
- 941 70. **He HH, Meyer CA, Chen MW, Jordan VC, Brown M, Liu XS.** Differential DNase I  
 942 hypersensitivity reveals factor-dependent chromatin dynamics. *Genome Res*. 2012;22:1015-1025.
- 943 71. **Spicuglia S, Vanhille L.** Chromatin signatures of active enhancers. *Nucleus*. 2012;3:126-131.
- 944 72. **Cheng J, Blum R, Bowman C, Hu D, Shilatifard A, Shen S, Dynlacht BD.** A role for H3K4  
 945 monomethylation in gene repression and partitioning of chromatin readers. *Mol Cell*.  
 946 2014;53:979-992.
- 947 73 **Chen WS, Manova K, Weinstein DC, Duncan SA, Plump AS, Prezioso VR, Bachvarova RF,**  
 948 **Darnell JE Jr.** Disruption of the HNF-4 gene, expressed in visceral endoderm, leads to cell

- 949 death in embryonic ectoderm and impaired gastrulation of mouse embryos. *Genes Dev.*  
 950 1994;8:2466-77.
- 951 74. **Lee CS, Friedman JR, Fulmer JT, Kaestner KH.** The initiation of liver development is  
 952 dependent on Foxa transcription factors. *Nature.* 2005;435:944-947.
- 953 75. **Bochkis IM, Schug J, Ye DZ, Kurinna S, Stratton SA, Barton MC, Kaestner KH.** Genome-  
 954 wide location analysis reveals distinct transcriptional circuitry by paralogous regulators Foxa1  
 955 and Foxa2. *PLoS Genet.* 2012;8:e1002770.
- 956 76. **Alder O, Cullum R, Lee S, Kan AC, Wei W, Yi Y, Garside VC, Bilenky M, Griffith M,**  
 957 **Morrissy AS, Robertson GA, Thiessen N, Zhao Y, Chen Q, Pan D, Jones SJ, Marra MA,**  
 958 **Hoodless PA.** Hippo signaling influences HNF4A and FOXA2 enhancer switching during  
 959 hepatocyte differentiation. *Cell Rep.* 2014;9:261-71
- 960 77. **Gordillo M, Evans T, Gouon-Evans V.** Orchestrating liver development. *Development.*  
 961 2015;142:2094-108.
- 962 78. **Sladek FM, Darnell JE.** Mechanisms of liver-specific gene expression. *Curr Opin Genet Dev.*  
 963 1992;2:256-9.
- 964 79. **Zaret KS.** Regulatory phases of early liver development: paradigms of organogenesis. *Nat Rev*  
 965 *Genet.* 2002;3:499-512.
- 966 80. **Shin D, Monga SP.** Cellular and molecular basis of liver development. *Compr Physiol.*  
 967 2013;3:799-815.
- 968 81. **Szklarczyk D, Franceschini A, Wyder S, Forslund K, Heller D, Huerta-Cepas J, Simonovic**  
 969 **M, Roth A, Santos A, Tsafou KP, Kuhn M, Bork P, Jensen LJ, von Mering C.** STRING v10:  
 970 protein-protein interaction networks, integrated over the tree of life. *Nucleic Acids Res.*  
 971 2015;43:D447-52.
- 972 82. **Holmes KA, Song JS, Liu XS, Brown M, Carroll JS.** Nkx3-1 and LEF-1 function as  
 973 transcriptional inhibitors of estrogen receptor activity. *Cancer Research* 2008;68:7380–85
- 974 83. **Jones ME, Boon WC, Proietto J, Simpson ER.** Of mice and men: the evolving phenotype of  
 975 aromatase deficiency. *Trends Endocrinol Metab.* 2006;17:55-64.

- 976 84. **Valéra MC, Gratacap MP, Gourdy P, Lenfant F, Cabou C, Toutain CE, Marcellin M, Saint**  
 977 **Laurent N, Sié P, Sixou M, Arnal JF, Payrastre B.** Chronic estradiol treatment reduces platelet  
 978 responses and protects mice from thromboembolism through the hematopoietic estrogen receptor  
 979  $\alpha$ . *Blood*. 2012;120:1703-1712.
- 980 85. **Mizuguchi T, Mitaka T, Hirata K, Oda H, Mochizuki Y.** Alteration of expression of liver-  
 981 enriched transcription factors in the transition between growth and differentiation of primary  
 982 cultured rat hepatocytes. *J Cell Physiol*. 1998;174:273-284.
- 983 86. **Chang TT, Hughes-Fulford M.** Molecular mechanisms underlying the enhanced functions of  
 984 three-dimensional hepatocyte aggregates. *Biomaterials*. 2014;35:2162-2171.
- 985 87. **Jagannathan V, Robinson-Rechavi M.** Meta-analysis of estrogen response in MCF-7  
 986 distinguishes early target genes involved in signaling and cell proliferation from later target  
 987 genes involved in cell cycle and DNA repair. *BMC Syst Biol*. 2011;5:138.
- 988 88. **Simpson NE, Gertz J, Imberg K, Myers RM, Garabedian MJ.** Research resource: enhanced  
 989 genome-wide occupancy of estrogen receptor  $\alpha$  by the cochaperone p23 in breast cancer cells.  
 990 *Mol Endocrinol*. 2012;26:194-202.
- 991 89. **Cavalli G, Misteli T.** Functional implications of genome topology. *Nat Struct Mol Biol*.  
 992 2013;20:290-299.
- 993 90. **Fullwood MJ, Liu MH, Pan YF, Liu J, Xu H, Mohamed YB, Orlov YL, Velkov S, Ho A,**  
 994 **Mei PH, Chew EG, Huang PY, Welboren WJ, Han Y, Ooi HS, Ariyaratne PN, Vega VB,**  
 995 **Luo Y, Tan PY, Choy PY, Wansa KD, Zhao B, Lim KS, Leow SC, Yow JS, Joseph R, Li H,**  
 996 **Desai KV, Thomsen JS, Lee YK, Karuturi RK, Herve T, Bourque G, Stunnenberg HG,**  
 997 **Ruan X, Cacheux-Rataboul V, Sung WK, Liu ET, Wei CL, Cheung E, Ruan Y.** An  
 998 oestrogen-receptor-alpha-bound human chromatin interactome. *Nature*. 2009;462:58-64.
- 999 91. **Ciabrelli F, Cavalli G.** Chromatin-driven behavior of topologically associating domains. *J Mol*  
 1000 *Biol*. 2015;427:608-625.
- 1001 92. **Zhang Y, Wong CH, Birnbaum RY, Li G, Favaro R, Ngan CY, Lim J, Tai E, Poh HM,**  
 1002 **Wong E, Mulawadi FH, Sung WK, Nicolis S, Ahituv N, Ruan Y, Wei CL.** Chromatin

- connectivity maps reveal dynamic promoter-enhancer long-range associations. *Nature*. 2013;504:306-310.
93. **Schoenfelder S, Furlan-Magaril M, Mifsud B, Tavares-Cadete F, Sugar R, Javierre BM, Nagano T, Katsman Y, Sakthidevi M, Wingett SW, Dimitrova E, Dimond A, Edelman LB, Elderkin S, Tabbada K, Darbo E, Andrews S, Herman B, Higgs A, LeProust E, Osborne CS, Mitchell JA, Luscombe NM, Fraser P.** The pluripotent regulatory circuitry connecting promoters to their long-range interacting elements. *Genome Res*. 2015;25:582-597.
94. **de Laat W, Duboule D.** Topology of mammalian developmental enhancers and their regulatory landscapes. *Nature*. 2013;502:499-506.
95. **Yi P, Wang Z, Feng Q, Pintilie GD, Foulds CE, Lanz RB, Ludtke SJ, Schmid MF, Chiu W, O'Malley BW.** Structure of a biologically active estrogen receptor-coactivator complex on DNA. *Mol Cell*. 2015;57:1047-1058.
96. **Flouriot G, Brand H, Denger S, Métivier R, Kos M, Reid G, Sonntag-Buck V, Gannon F.** Identification of a new isoform of the human estrogen receptor-alpha (hER-alpha) that is encoded by distinct transcripts and that is able to repress hER-alpha activation function 1. *EMBO J*. 2000;19:4688-4700.
97. **Wang Z, Zhang X, Shen P, Loggie BW, Chang Y, Deuel TF.** Identification, cloning, and expression of human estrogen receptor-alpha36, a novel variant of human estrogen receptor-alpha66. *Biochem Biophys Res Commun*. 2005;336:1023-1027.
98. **Irsik DL, Carmines PK, Lane PH.** Classical estrogen receptors and ER $\alpha$  splice variants in the mouse. *PLoS One*. 2013;8:e70926.
99. **John S, Sabo PJ, Thurman RE, Sung MH, Biddie SC, Johnson TA, Hager GL, Stamatoyannopoulos JA.** Chromatin accessibility pre-determines glucocorticoid receptor binding patterns. *Nat Genet*. 2011;43:264-268.
100. **Theodorou V, Stark R, Menon S, Carroll JS.** GATA3 acts upstream of FOXA1 in mediating ESR1 binding by shaping enhancer accessibility. *Genome Res*. 2013;23:12-22.
101. **Mo R, Rao SM, Zhu YJ.** Identification of the MLL2 complex as a coactivator for estrogen receptor alpha. *J Biol Chem*. 2006;281:15714-15720.



- 1031 102. **Kim H, Heo K, Kim JH, Kim K, Choi J, An W.** Requirement of histone methyltransferase  
 1032 SMYD3 for estrogen receptor-mediated transcription. *J Biol Chem.* 2009;284:19867-19877.
- 1033 103. **Shi L, Sun L, Li Q, Liang J, Yu W, Yi X, Yang X, Li Y, Han X, Zhang Y, Xuan C, Yao**  
 1034 **Z, Shang Y.** Histone demethylase JMJD2B coordinates H3K4/H3K9 methylation and promotes  
 1035 hormonally responsive breast carcinogenesis. *Proc Natl Acad Sci USA.* 2011;108:7541-7546.
- 1036 104. **Jeong KW, Andreu-Vieyra C, You JS, Jones PA, Stallcup MR.** Establishment of active  
 1037 chromatin structure at enhancer elements by mixed-lineage leukemia 1 to initiate estrogen-  
 1038 dependent gene expression. *Nucleic Acids Res.* 2014;42:2245-2256.
- 1039 105. **Zhang X, Tanaka K, Yan J, Li J, Peng D, Jiang Y, Yang Z, Barton MC, Wen H, Shi,X.**  
 1040 Regulation of estrogen receptor  $\alpha$  by histone methyltransferase SMYD2-mediated protein  
 1041 methylation. *Proc Natl Acad Sci USA.* 2013;110:17284-17289.
- 1042 106. **Jiang Y, Trescott L, Holcomb J, Zhang X, Brunzelle J, Sirinupong N, Shi X, Yang Z.**  
 1043 Structural insights into estrogen receptor  $\alpha$  methylation by histone methyltransferase SMYD2, a  
 1044 cellular event implicated in estrogen signaling regulation. *J Mol Biol.* 2014;426:3413-3425.
- 1045 107. **Formosa T.** The role of FACT in making and breaking nucleosomes. *Biochim Biophys Acta.*  
 1046 2013;1819:247-255.
- 1047 108. **Gurard-Levin ZA, Quivy JP, Almouzni G.** Histone chaperones: assisting histone traffic and  
 1048 nucleosome dynamics. *Annu Rev Biochem.* 2014;83:487-517.
- 1049 109. **Edwards DP.** Regulation of signal transduction pathways by estrogen and progesterone.  
 1050 *Annu Rev Physiol.* 2005;67:335-376.
- 1051 110. **Arao Y, Hamilton KJ, Ray MK, Scott G, Mishina Y, Korach KS.** Estrogen receptor  $\alpha$  AF-  
 1052 2 mutation results in antagonist reversal and reveals tissue selective function of estrogen receptor  
 1053 modulators. *Proc Natl Acad Sci USA.* 2011;108:14986-14991.
- 1054 111. **Billon-Galés A, Krust A, Fontaine C, Abot A, Flouriot G, Toutain C, Berges H, Gadeau**  
 1055 **AP, Lenfant F, Gourdy P, Chambon P, Arnal, JF.** Activation function 2 (AF2) of estrogen  
 1056 receptor- $\alpha$  is required for the atheroprotective action of estradiol but not to accelerate  
 1057 endothelial healing. *Proc Natl Acad Sci USA.* 2011;108:13311-13316.



- 1058 112. **Adlanmerini M, Solinhac R, Abot A, Fabre A, Raymond-Letron I, Guihot AL, Boudou**  
1059 **F, Sautier L, Vessières E, Kim SH, Lière P, Fontaine C, Krust A, Chambon P,**  
1060 **Katzenellenbogen JA, Gourdy P, Shaul PW, Henrion D, Arnal JF, Lenfant F.** Mutation of  
1061 the palmitoylation site of estrogen receptor  $\alpha$  in vivo reveals tissue-specific roles for membrane  
1062 versus nuclear actions. *Proc Natl Acad Sci USA*. 2014;111:E283-290.
- 1063 113. **Pedram A, Razandi M, Lewis M, Hammes S, Levin ER.** Membrane-localized estrogen  
1064 receptor  $\alpha$  is required for normal organ development and function. *Dev Cell*. 2014;29:482-490.  
1065  
1066

## FIGURE LEGENDS

**Figure 1.** Characterization of the E2-dependent genes in livers from ERWT and ERKO mice. A, Heatmap illustrating the mean expression values determined for E2-sensitive genes (left side) in placebo- (P) and 17 $\beta$  estradiol (E2)-treated ERWT animals or for genes whose expression was different between placebo-treated ERWT and ERKO mice (right side). Each column corresponds to data obtained for one animal. For the sake of clarity, expression values for each gene were normalized by the mean and standard deviation. The percentages of up- and down-regulated genes are indicated on the sides of each heatmap. B, Venn diagram depicting the overlap between genes regulated by E2 in ERWT livers and genes whose expression differed between ERWT and ERKO mice.

**Figure 2.** Characterization of the ER cistrome in mouse liver. A, ER ChIP-seq experiments were performed on chromatin prepared from placebo- (P) or E2-treated ERWT and ERKO livers. We systematically used different *p*-values at the peak-calling step to determine the ER cistrome under the different conditions. This panel represents the number of identified ER BSs as a function of the *p*-values used. The color code used in panel A is the same for the next ones. B, Overlap of the different ER cistromes obtained at diverse *p*-values. C, Venn diagram illustrating the common and specific ER BSs using ER cistromes determined at a *p*-value of 10<sup>-5</sup>. D, Heatmap representation of the ChIP-seq signal aligned to the center of ER BSs clustered depending on their overlap determined in panel C. E, Mean ER ChIP-seq signals obtained in ERWT or ERKO mouse livers at the 150 center base pairs of the BSs categories indicated beneath the graph. The upper histogram shows mean values  $\pm$  SD measured on the sites of interest whilst the bottom graph shows mean values  $\pm$  SD of 10 trials carried out on 10 different sets of a corresponding number of random sites.

**Figure 3.** Validation of ER BSs. (A and B) ER ChIP-qPCR experiments were performed on livers from independent animals (numbers on the top of the panel) to validate ChIP-seq data. In Panel A, a fraction of the pool of DNA that was subjected to high-throughput sequencing (HTS) was used as a control. We used two panels of antibody: one directed against the C-terminal region of ER (left side of panels A and B) and the other targeting the N-terminal domain of the protein (A and B, right side). The mobilization of ER was evaluated on a series of genomic regions representing clusters of ER BSs engaged by ER in the presence of E2 or not (#1) or BSs specific for ERKO (#2) or ERWT P (#3)

conditions. The results of these experiments are illustrated as a heatmap of values normalized to those of the promoter of the *Rplp0* gene, which is an ER-negative region. We also used additional negative and positive controls, located nearby the E2-sensitive *Gdf15* gene: *Gdf15.2* and *Gdf15.3*, respectively. In panel B, the results of the experiments were hierarchically clustered to improve the clarity of the heatmap. The distance metric expressed as Pearson correlation is indicated on the right side of the panel. N.D stands for not determined.

**Figure 4.** Specific features of the ER cistrome in mouse liver. A, Distribution of ER BSs determined in E2- or placebo-treated ERWT mouse liver towards annotated gene promoters and TTSs, exons and introns, and intergenic (distal) regions. B, Number of ER BSs located within a 1kb or 3kb window around the TSS of annotated genes in ERWT (P+E2) mouse liver when compared to ER binding data obtained in human breast cancer MCF-7 cells. Calculations were also made using an equivalent number of random regions with similar characteristics than the test ER cistrome determined in ERWT livers. C, Bar chart summarizing the distribution of distances separating E2-regulated genes in breast cancer cell lines or in ERWT mice liver or ER-dependent genes from their closest ER BS. Results are expressed as the percentage of the total population of genes considered. D, Fold-changes in gene expression by E2 in MCF-7 and ERWT mouse liver and in ERKO vs. ERWT liver are expressed as a function of their proximity to an ER BS. Distribution of values are depicted within the left part of the panel, while means  $\pm$  SD are plotted on the right side of the panel.

**Figure 5.** Coordinated changes in H3K4me2 and H3K27ac levels at promoters of ER-dependent genes. A, Alignment of H3K4me2 and H3K27ac ChIP-seq signals generated from chromatin prepared from E2-treated livers of ERWT (red line) or ERKO (blue line) mice on a -5kbp/+5kbp window around the center of the ER BSs. B and C, Mean H3K4me2 and H3K27ac ChIP-seq signals at a -500/+500 bp window around the center of ERBSs (B) or within a 4 kb window centered around the TSS of genes with lower or higher expression in ERKO livers (down-or up-regulated, respectively). D, The fold-change of mean H3K27 values calculated for each of the promoters of down-or up-regulated genes in ERKO livers are plotted against variations of mean H3K4me2 signals. Values shown are expressed as the log2 of the fold-changes.

**Figure 6.** Affected profile of H3K4me2 enrichment of a fraction of ERBSs in ERKO livers. A, Heatmap representation of a k-mean clusterization of H3K4me2 and H3K27ac ChIP-seq signals obtained in ERWT and ERKO mice livers on ERWT ER BSs. The distribution of clustered ER BSs towards annotated genes' transcriptional start and termination sites (TSS and TTS, respectively), intragenic and intergenic (Distal) regions is indicated on the right side of each clusters, as well as the numbers of genomic sites within each cluster. B, Alignments of H3K4me2 and H3K27ac ChIP-seq mean signals within a -5kbp/+5kbp window centered on ER BSs of each clusters as defined from the k-mean analysis. Signals obtained in E2-treated livers of ERWT or ERKO mice are illustrated as a red or blue line, respectively. Insets represent magnified views of the center of the graphs and illustrate the observed shift from biphasic to monophasic curves of enrichment in H3K4me2.

**Figure 7.** Chromatin status of ER BSs in ERWT and ERKO mouse livers. A, Independent anti-H3K4me1, H3K4me2 and H3K27ac ChIP-qPCR experiments were performed to validate ChIP-seq data. The presence of these marks on ER BSs from series #1 and #3, as defined in Fig. 3, is depicted within the illustrated heatmaps. Numbers on the top refer to the animals from which the chromatin preparations originated. Experiments were done twice per individual. Mean enrichment values calculated per individual are shown as normalized to a control negative ChIP experiment using the same chromatin samples. B, Heatmap illustrating the mean enrichment of indicated ER BSs in 5-mC and 5-hmC as tested by MeDIP- and hMeDIP-qPCR experiments, respectively. The values included within these graphs were obtained from three independent experiments performed on two different DNA samples originating from two different ERWT or ERKO animals. Data were normalized to values obtained using an internal negative control devoid of CpGs. Significant reduced (green) or gained (red) enrichment in histone marks or DNA modifications ERKO livers are indicated in the heatmaps on the right side of each panels. Calculated *p*-values from Mann-Whitney *t*-tests are indicated within the heatmap as follows: \* $< 0.05$ ; \*\* $< 0.01$ .

**Figure 8.** Overlap of ER and Hnf4 $\alpha$  cistromes. A, Overlap of the ER BSs determined in E2-treated ERWT livers with those of Hnf4 $\alpha$  obtained at diverse *p*-values. B, Heatmap representation of ER and Hnf4 $\alpha$  ChIP-seq signals within a -5kbp/+5kbp window centered on ER BSs. Regions are sorted by their rank in ER ChIP-seq signal. C, Heatmap representing the overlap between the clusters of ER

BSs as determined in Fig. 6 with Hnf4a BSs determined at a  $p$ -value of  $10^{-5}$ . The numbers indicated represent the calculated overlaps.

**Figure 9.** The Foxa2 cistrome is partially ER-dependent. A, Foxa2 ChIP-seq experiments were performed on chromatin prepared from E2-treated ERWT and ERKO livers. As carried out previously, we systematically used different thresholds to determine the number of Foxa2 BSs in each of the experimental conditions (orange and grey lines for ERWT and ERKO animals respectively). The number of ER BSs in ERWT (red curve) is given as reference. The color code used in panel A is the same for the next ones. B, Overlap of the different Foxa2 cistromes at diverse  $p$ -values with ER BSs or Foxa2 BSs determined in E2-treated ERWT livers (left and middle graphs), or Foxa2 BSs in E2-treated ERKO livers (right). C, Venn diagram illustrating the overlap of ER BSs with Foxa2 BSs in ERWT or ERKO mice at the chosen  $p$ -value of  $10^{-4}$ . D, Heatmap of Foxa2 normalized ChIP-seq signals obtained from ERWT or ERKO chromatin on conserved, lost or gained Foxa2 BSs. E, Mean Foxa2 ChIP-seq signals obtained in ERWT or ERKO mouse livers (orange or grey bars, respectively) at the 150 center base pairs of Foxa2 BSs. The upper histogram shows mean values  $\pm$  SD measured for conserved, gained or lost sites. Calculations were also carried out for 10 different sets of a corresponding number of random sites. Means  $\pm$  SD of these 10 random trials are illustrated within the bottom histogram. F, Anti-Foxa2 ChIP-qPCR experiments were performed on four liver chromatin samples originating from independent E2-treated ERWT or ERKO mice. A fraction of the pooled DNA sample that was subjected to HTS was also evaluated in parallel. The upper heatmap shows the values obtained on indicated tested genomic regions normalized to those obtained from a non-specific control (promoter of the *Rplp0* gene) and to the control ChIP sample. Significant reduced (green) or gained (red) mobilization of Foxa2 in ERKO livers is indicated in the lower heatmap. Calculated  $p$ -values from Mann-Whitney  $t$ -tests are indicated as follows: \* $< 0.05$ ; \*\* $< 0.01$ .

**Figure 10.** Chromatin status of Foxa2 BSs in ERWT and ERKO mouse livers. A and B, Alignment of mean H3K4me2 (left side of the panel) or H3K27ac signals on categorized Foxa2 BSs. Insets represent magnified views of the center of the graphs and illustrate the observed shift from biphasic to monophasic curves of enrichment in H3K4me2. C, Heatmap representation of results obtained in independent anti H3K4me1, H3K4me2 and H3K27ac ChIP-qPCR experiments. The presence of these

marks was followed in livers from ERWT and ERKO animals (numbers on the right refer to individuals) at the indicated conserved or lost Foxa2 BSs. Experiments were done twice per individual. Mean fold enrichment values shown are expressed as relative to a control negative ChIP experiment using the same chromatin samples. D, Summary of MeDIP- and hMeDIP-qPCR assays, illustrated as in panel B. The values included within these graphs were obtained in three independent experiments performed on two different DNA samples originating from two different ERWT or ERKO animals. Significant reduced (green) or gained (red) enrichment in histone marks or DNA modifications in ERKO livers are indicated in the lower heatmaps. Calculated *p*-values from Mann-Whitney *t*-tests are indicated as follows: \* $< 0.05$ ; \*\* $< 0.01$ .

**Figure 11.** Multiple TFs may protect Foxa2 BSs from loss-of function in ERKO livers. A, Wordle graphics (<http://www.wordle.net/website>) of enriched motifs for transcription factors binding within lost Foxa2 BSs; as determined by the SeqPos algorithm (<http://cistrome.org/ap/>). B, Overlap of categorized Foxa2 BSs with the cistromes of different transcription factors, all determined in mouse liver except Nkx3-1 BSs which were identified in mouse prostate.

**Table 1.** E2- and ER-dependent liver transcriptomes associated functions.

		Description	adjP
GO Biological Processes	E2-sensitive	lipid metabolic process	0.063
		regulation of fibroblast growth factor receptor signaling pathway	0.063
		fibroblast growth factor receptor signaling pathway	0.063
		negative regulation of cellular response to growth factor stimulus	0.063
		negative regulation of fibroblast growth factor receptor signaling pathway	0.063
		alcohol metabolic process	0.063
		intracellular signal transduction	0.063
		enzyme linked receptor protein signaling pathway	0.063
		small molecule metabolic process	0.078
		organic substance metabolic process	0.078
		cellular response to fibroblast growth factor stimulus	0.078
		polyol metabolic process	0.078
		response to fibroblast growth factor stimulus	0.078
	ER-dependent (-E2)	negative regulation of biological process	0.0008
		growth	0.0008
		oxidation-reduction process	0.0008
		negative regulation of cellular process	0.0014
		mammary gland development	0.0014
		regulation of growth	0.0020
		mammary gland alveolus development	0.0052
		mammary gland lobule development	0.0052
		developmental process	0.0052
		positive regulation of cell differentiation	0.0052
		metabolic process	0.0052
		multicellular organismal development	0.0081
		reactive oxygen species metabolic process	0.0081
		negative regulation of growth	0.0081
		lipid metabolic process	0.0090
		positive regulation of reactive oxygen species metabolic process	0.0090
		single-organism metabolic process	0.0090
		positive regulation of developmental process	0.0090
		positive regulation of glucose import	0.0090
		organ development	0.0091
		regulation of body fluid levels	0.0091
		system development	0.0091
		anatomical structure development	0.0091
		regulation of glucose metabolic process	0.0091
		gastrulation with mouth forming second	0.0091
Pathways	E2-sensitive	Adipogenesis (Wiki)	0.0021
		Metabolic pathways (Kegg)	0.0024
		Cytokine-cytokine receptor interaction (Kegg)	0.0036
	ER-dependent (-E2)	Adipogenesis (Wiki)	6.53e-06
		IL-3 Signaling (Wiki)	2.97e-05
		Leptin Insulin Overlap (Wiki)	5.94e-05
		ErbB signaling (Wiki)	0.0008
		PPAR signaling (Wiki)	0.0022
		IL-6 signaling (Wiki)	0.0032
		Amino Acid metabolism (Wiki)	0.0032
		Androgen Receptor Signaling (Wiki)	0.0035
		Metabolic pathways (Kegg)	2.43e-08
		Adipocytokine signaling (Kegg)	0.0001
		Glycine, serine and threonine metabolism (Kegg)	0.0003
		Fatty acid metabolism (Kegg)	0.0005
		Type II diabetes mellitus (Kegg)	0.0005
		Jak-STAT signaling pathway (Kegg)	0.0009
		Bile secretion (Kegg)	0.0011
		Retinol metabolism (Kegg)	0.0012
		PPAR signaling pathway (Kegg)	0.0012
		Arachidonic acid metabolism (Kegg)	0.0014
		Hepatitis C (Kegg)	0.0042
		Insulin signaling pathway (Kegg)	0.0042

Functional annotations are shown for GO Biological processes and for a compilation of Wiki and Kegg pathways. Adjusted Bonferroni p-values are indicated (adjP).



**Table 2.** Enriched DNA Motifs in identified ERBSs.

ERWT E2				ERWT P				ERKO			
CentDist		SeqPos		CentDist		SeqPos		CentDist		SeqPos	
Motif Family	Score	Factor	Z-Score	Motif Family	Score	Factor	Z-Score	Motif Family	Score	Factor	Z-Score
ERE	63.3457	ESR1	-54.177	ERE	19.8389	ESR1	-16.769	No Motif identified		SREBF1	-2.823
AR	27.5415	ESR2	-48.709	AR	9.2016	ESR2	-15.407			E2F6	-2.55
CEBP	19.9196	NR1H4	-41.196	SP1	7.07288	PPARG	-10.533				
CREB	17.3222	NR2F1	-38.985	CREB	6.725	Nr1d2	-9.025				
NF1	14.969	Nr1d2	-35.506	AP2	6.55955	PPARG::RXRA	-7.921				
FOX	14.6542	Rxra	-34.347	NRF	6.27122	Rxra	-7.705				
LRH1	14.6223	PPARG	-30.851	E2F	6.00375	NR1H4	-7.519				
SP1	13.5031	PPARA	-30.684	MINI	5.66217	NR2F1	-7.021				
PAX	13.3069	Esrrb	-28.943	HIC1	5.1859	RORB	-6.933				
E2F	13.2217	Nr1d1	-27.169	CEBP	5.1783	Nr1d1	-6.739				
FXR	12.0634	Nr2f2	-25.821	ETS	5.10736	PPARA	-6.595				
AP4	12.014	RORB	-25.117	EGR	5.08289	AR	-4.809				
AP2	11.8928	RARA	-25.044	SP3	5.00439	Zscan10	-4.476				
HIC1	11.8863	PPARG::RXRA	-24.754	ZF5	4.87866	Zfp161	-4.295				
HEN	11.097	ESRRA	-23.913	P53	4.82231	EGR3	-4.147				
AP1	10.8325	Hnf4a	-23.697	LMAF	4.81312	HMG1	-4.1				
ARP1	10.6548	NR0B1	-22.347	NF1	4.71645	ZSCAN4	-4.014				
ZF5	10.6078	RXRB	-21.033	EBOX	4.64247	NR3C1	-3.894				
MEF3	10.5625	NR4A1	-20.62	GGG	4.44056	Rarg	-3.742				
MINI	10.5463	NR2C2	-20.308	FOX	4.33386	NR0B1	-3.544				
EBOX	10.5284	Rxrg	-20.177	CP2	4.1856	GMEB2	-3.438				
MIF1	10.3304	RORA	-20.112	SMAD	4.04632	NR2C2	-3.433				
GGG	10.2881	Rarg	-19.838	EBF	3.95207	EGR4	-3.42				
SMAD	10.1529	Nr5a2	-19.729	DEAF1	3.93445	Esrrb	-3.401				
LEF	9.80931	Cebpb	-18.033	PAX	3.88007	E2F3	-3.353				
HNF1	9.73785	Cebpa	-17.783	CAAT	3.86651	MTF1	-3.329				
HNF6	9.55107	CEBPE	-17.524	HEN	3.86643	NR3C2	-3.179				
ATCGAT	9.48478	SF1	-16.74	STAT	3.81298	RXR	-3.161				
BACH	9.09395	AR	-16.689	AP4	3.76367	PAX2	-3.14				
CACCC	9.07574	NR6A1	-16.346	DBP	3.75713	Maf	-3.116				
DBP	8.80169	CEBPD	-16.334	SRF	3.58963	E2F2	-3.069				
NRF	8.75417	THRB	-15.294	KAISO	3.5676	TP63	-2.723				
VMAF	8.74793	CEBPG	-15.105	CACCC	3.55511	PGR	-2.622				
P53	8.57691	NR3C1	-14.897	MEIS1	3.54119	NANOG	-2.603				
LMAF	8.54137	VDR	-14.558	IK	3.32866	VDR	-2.529				
CAAT	8.30663	NR3C2	-14.523	LRH1	3.1906	Egr2	-2.509				
CP2	8.17824	NR2F6	-14.179	WT1	3.17195						
		NR4A2	-14.073	ZNF219	3.14613						
		ESRRG	-13.415	RFX	3.0712						
		ATF2	-13.373	STAF	2.9954						
		ATF2::JUN	-13.185								
		ATF6	-12.984								
		THRA	-12.737								
		Jdp2	-12.54								
		THRB	-12.515								
		CREB3	-11.811								
		RARB	-11.735								
		NFIX	-11.73								
		NFIB	-11.623								
		ATF4	-10.996								
		NR2E3	-10.893								
		Creb5	-10.694								
		PAX2	-10.551								
		ATF1	-10.415								
		NFIC	-10.269								
		BATF3	-10.214								
		ATF7	-10.207								
		Foxa2	-9.851								
		PGR	-9.837								
		FOXA1	-9.831								
		Creb3l2	-9.414								
		NR112	-9.322								
		NFIL3	-9.241								
		Pax3	-9.197								

Motif analysis was performed using CentDist (<http://biogpu.ddns.comp.nus.edu.sg/~chipseq/webseqtools2>) and SePos (<http://cistrome.org/ap/>) algorithms. Sequences were declared enriched by when p-value<0.05 and Z-score>2.5. Only the 65 best sequences characterized by SeqPos are shown for ERBSs identified in E2-treated ERWT animals. Full analyses are depicted in the Supplemental File 3.

**Table 3.** Functional annotations of genes proximal to ERBSs from ERWT livers.

	<b>Term</b>	<b>p-value</b>
<b>MGI Expression</b>	TS23_liver; lobe	4.22e-40
	TS26_liver	6.67e-32
	TS26_liver and biliary system	1.03e-31
	TS24_liver	1.56e-27
	TS24_liver and biliary system	2.66e-24
	TS15_septum transversum; hepatic component	1.11e-15
	TS23_adrenal gland; medulla	3.13e-13
<b>GO Biological Process</b>	organic acid metabolic process	3.69e-49
	carboxylic acid metabolic process	2.74e-48
	cellular ketone metabolic process	6.43e-48
	lipid metabolic process	7.95e-48
	cellular response to hormone stimulus	1.87e-43
	cellular response to peptide hormone stimulus	1.25e-40
	monocarboxylic acid metabolic process	7.54e-38
	cellular response to insulin stimulus	4.52e-37
	response to peptide hormone stimulus	7.26e-36
<b>GO Molecular Function</b>	response to insulin stimulus	2.78e-35
	lyase activity	7.09e-15
	monocarboxylic acid binding	4.91e-14
	heme binding	2.99e-13
	apolipoprotein binding	6.24e-13
	transferring acyl groups	5.44e-11
	carboxylic acid binding	1.85e-12
	steroid binding	5.63e-12
	vitamin binding	2.74e-11
	steroid hydroxylase activity	1.69e-10
<b>Mouse Phenotype</b>	ligand-regulated transcription factor activity	1.02e-09
	abnormal lipid homeostasis	9.28e-75
	abnormal lipid level	1.01e-71
	abnormal circulating lipid level	8.51e-70
	abnormal liver physiology	8.41e-63
	abnormal hepatobiliary system physiology	8.27e-62
	abnormal triglyceride level	4.24e-61
	decreased cholesterol level	1.01e-52
	abnormal circulating cholesterol level	5.19e-52
	abnormal cholesterol level	1.09e-51
	abnormal cholesterol homeostasis	4.65e-50

Functional annotations were determined by GREAT [<http://bejerano.stanford.edu/great/public/html/index.php> (51)] using basic parameters (basal criteria for associating genomic regions with genes).

**Table 4.** Enriched DNA Motifs in categorized FoxA2 BSs.

Conserved		Gained		Lost	
Factor	Z-Score	Factor	Z-Score	Factor	Z-Score
Foxa2	-91.617	Foxa2	-23.414	Foxa2	-59.79
FOXA1	-90.958	FOXA1	-23.058	FOXA1	-59.536
FOX11	-81.908	FOX11	-22.795	FOX11	-56.216
Foxg1	-80.449	FOXB1	-21.524	Foxg1	-54.751
FOXB1	-78.905	FOXP1	-21.512	FOXP1	-52.788
FOXP1	-78.788	Foxg1	-21.297	Nkx3-1	-52.633
FOXD2	-75.482	Foxk1	-20.161	FOXB1	-50.984
FOXD3	-74.081	FOXL1	-19.777	FOXL1	-50.971
FOXL1	-73.89	FOXD2	-19.095	FOXD2	-48.341
Nkx3-1	-72.907	Nkx3-1	-18.785	FOXD3	-47.994
Foxk1	-72.123	FOXD3	-18.614	Foxk1	-47.988
FOXD1	-70.968	FOXD1	-17.878	FOXD1	-46.354
FOXC2	-67.3	FOXP3	-17.007	FOXP3	-44.639
FOXC1	-66.927	FOXO3	-16.517	FOXO3	-43.621
FOXO3	-66.241	FOXC2	-15.411	FOXC2	-39.98
FOXP3	-64.662	FOXC1	-14.102	FOXC1	-35.118
FOXF2	-51.748	FOXF2	-13.535	FOXF2	-34.484
Foxj1	-51.576	CEBPD	-12.481	Foxj1	-33.619
FOXJ3	-45.412	Cebpb	-12.292	Foxf1a	-29.292
Foxf1a	-40.616	CEBPE	-12.152	FOXJ3	-26.531
FOXH1	-32.447	Cebpα	-11.812	FOXH1	-22.446
CEBPE	-27.482	Foxj1	-11.6	Hnf4a	-15.71
Cebpb	-27.19	CEBPG	-11.278	Cebpb	-15.134
CEBPA	-26.856	FOXJ3	-9.067	CEBPA	-14.552
CEBPD	-26.765	Foxf1a	-8.978	CEBPE	-14.418
HNF4A	-26.219	Hnf4a	-8.801	CEBPD	-14.338
Foxq1	-24.216	FOXH1	-8.068	CEBPG	-13.844
CEBPG	-22.81	RXRB	-7.845	NR2C2	-13.376
FOXG1	-19.912	RXRA	-7.44	Rxb	-12.575
NR2C2	-19.459	NR2F6	-7.128	NR2F1	-11.973
FOXJ2	-19.292	PPARA	-7.113	Ppara	-11.972
RXRB	-19.023	HLF	-7.05	NR2F6	-11.776
NR2F6	-18.985	NFIL3	-6.95	NR1H4	-11.079
RARA	-17.842	RARA	-6.798	Nr1d2	-10.656
NR2F1	-17.813	NR2C2	-6.428	RARA	-10.297
Nr2f2	-16.99	DBP	-6.041	Foxq1	-10.091
NR1H4	-16.511	Nr1d2	-5.836	FOXJ2	-9.851
NR2E3	-16.142	ATF4	-5.821	Rxra	-9.762
NR4A1	-16.003	NR1H4	-5.659	NFIX	-9.739
Nr1d2	-15.912	NR2F1	-5.438	Nr2f2	-9.385
Ppara	-15.867	ZSCAN4	-5.432	ZSCAN4	-9.131
SRY	-15.493	Pparg	-4.988	NFIC	-8.927
ZNF435	-15.351	Nr2f2	-4.944	FOXO6	-8.69
NFIL3	-15.241	Creb5	-4.864	Zscan10	-8.445
ESRRA	-15.067	NFIB	-4.757	NR4A1	-8.393
ATF4	-14.596	ATF7	-4.756	ESRRA	-8.372
FOXO4	-14.388	TEF	-4.756	NFIB	-8.199
FOXO6	-13.684	NR2E1	-4.534	HEY1	-8.186
NFIC	-13.639	Foxq1	-4.379	NR2E3	-8.143
Rxra	-13.167	NFIX	-4.329	Esrrb	-8.116

Motif analysis was performed using SeqPos algorithm (<http://cistrome.org/ap/>). Sequences were declared enriched by when p-value<0.05 and Z-score>2.5. Only the best 50 sequences characterized are shown. Full analyses are depicted in the Supplemental File 3.

Figure 1

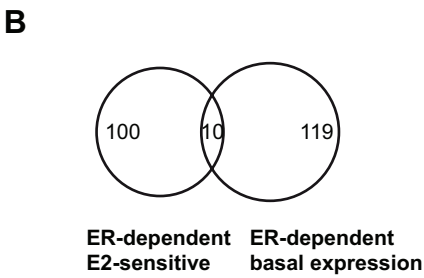
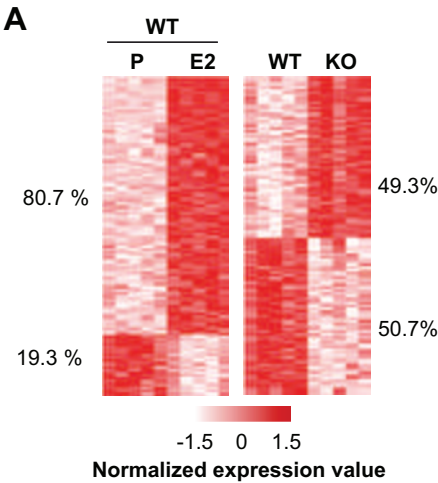


Figure 2

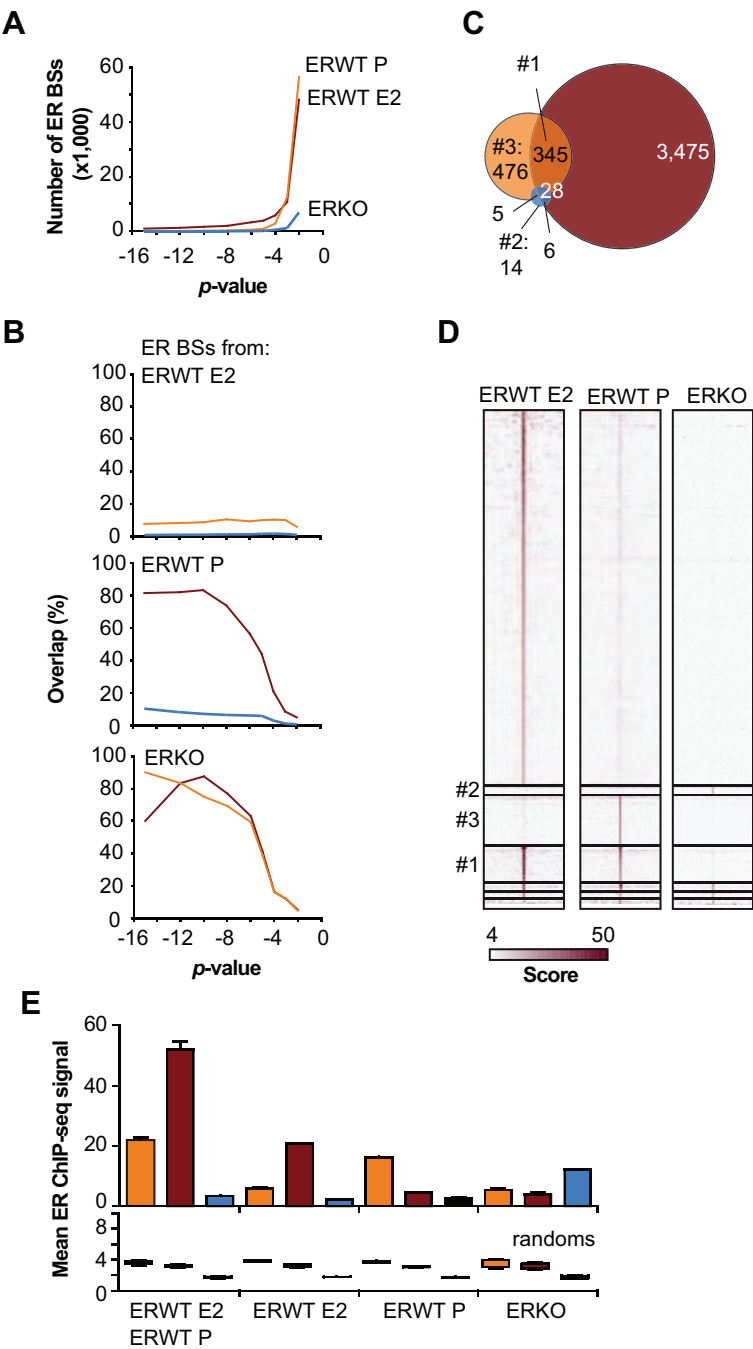
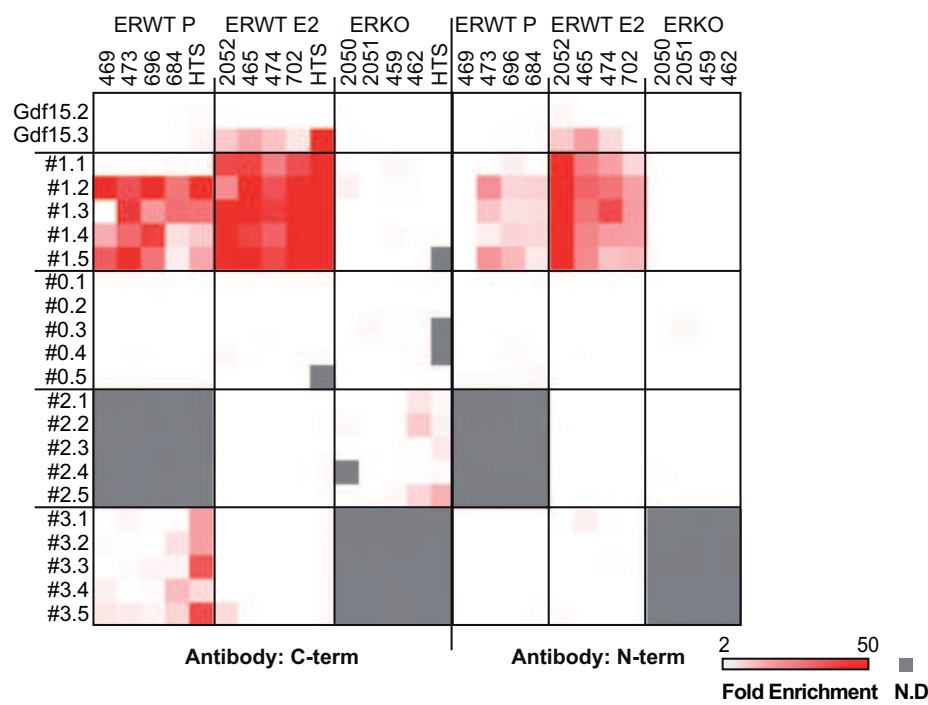


Figure 3

A



B

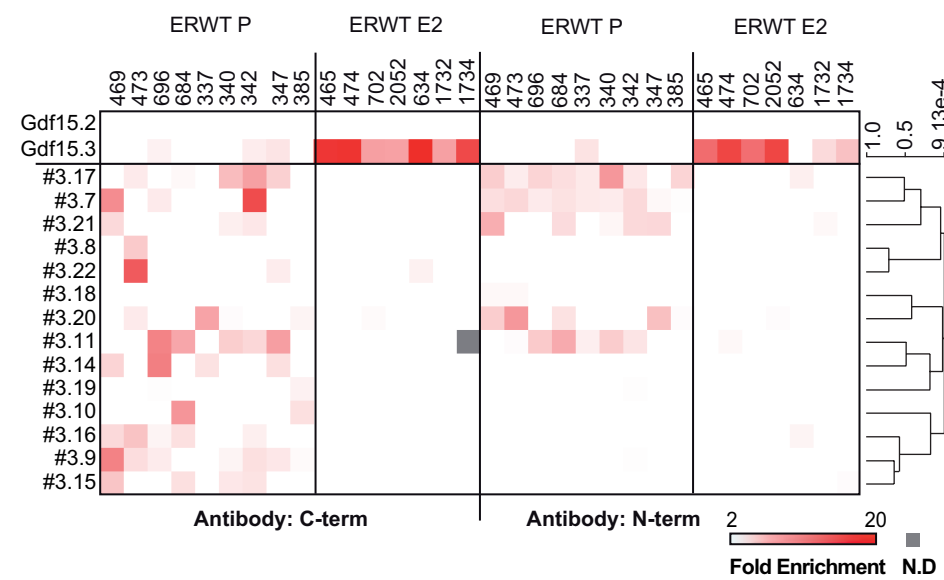


Figure 4

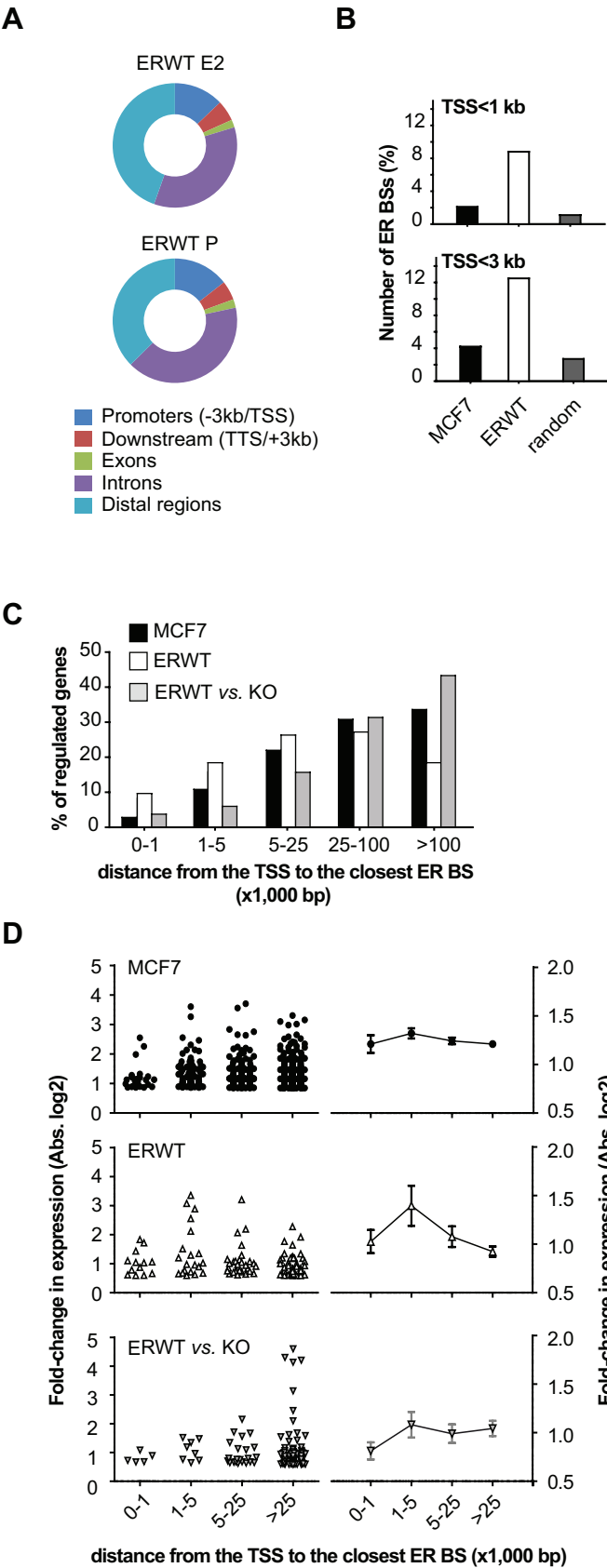




Figure 5

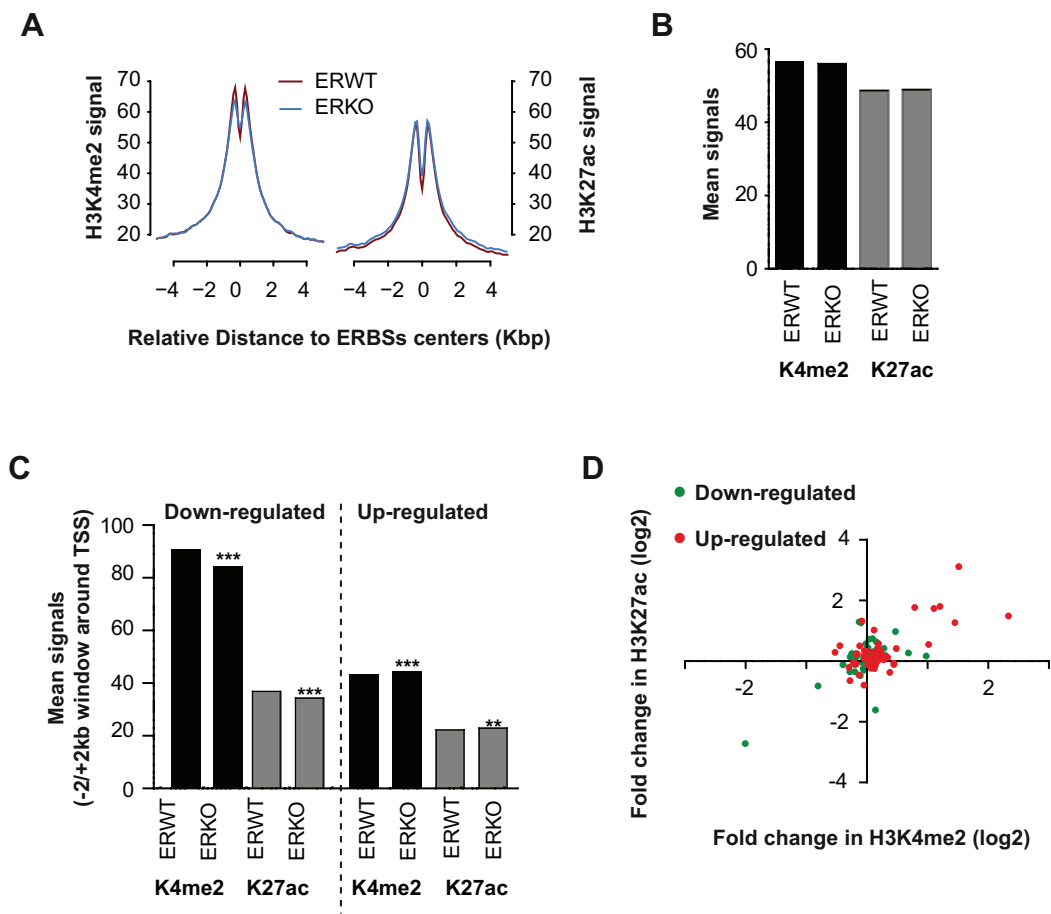


Figure 6

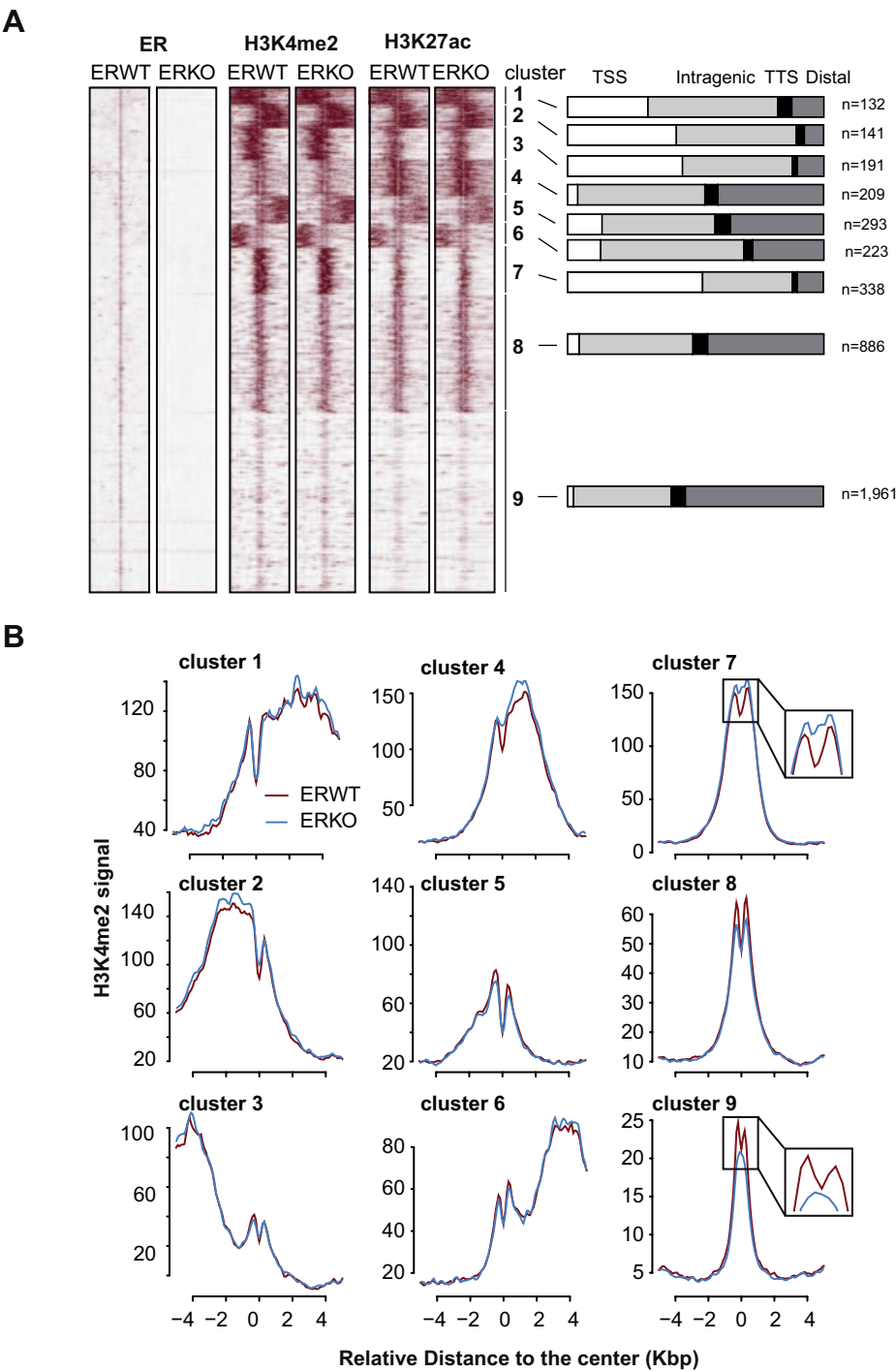


Figure 7

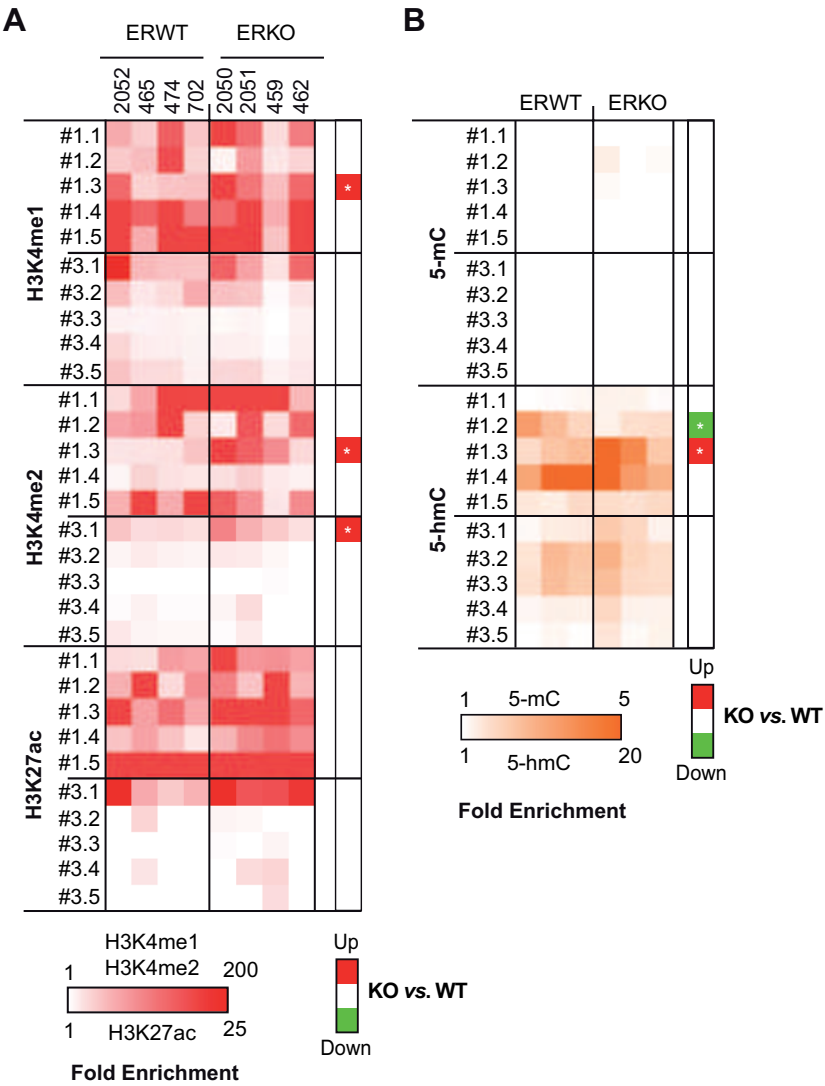


Figure 8

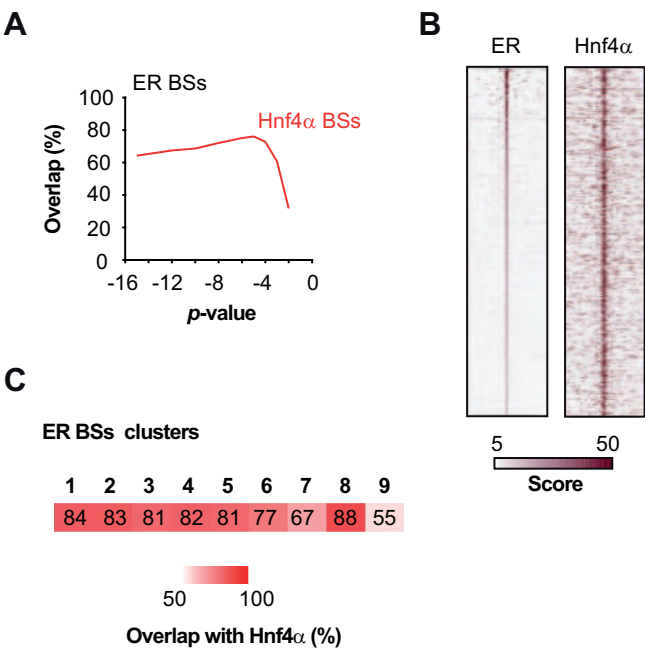


Figure 9

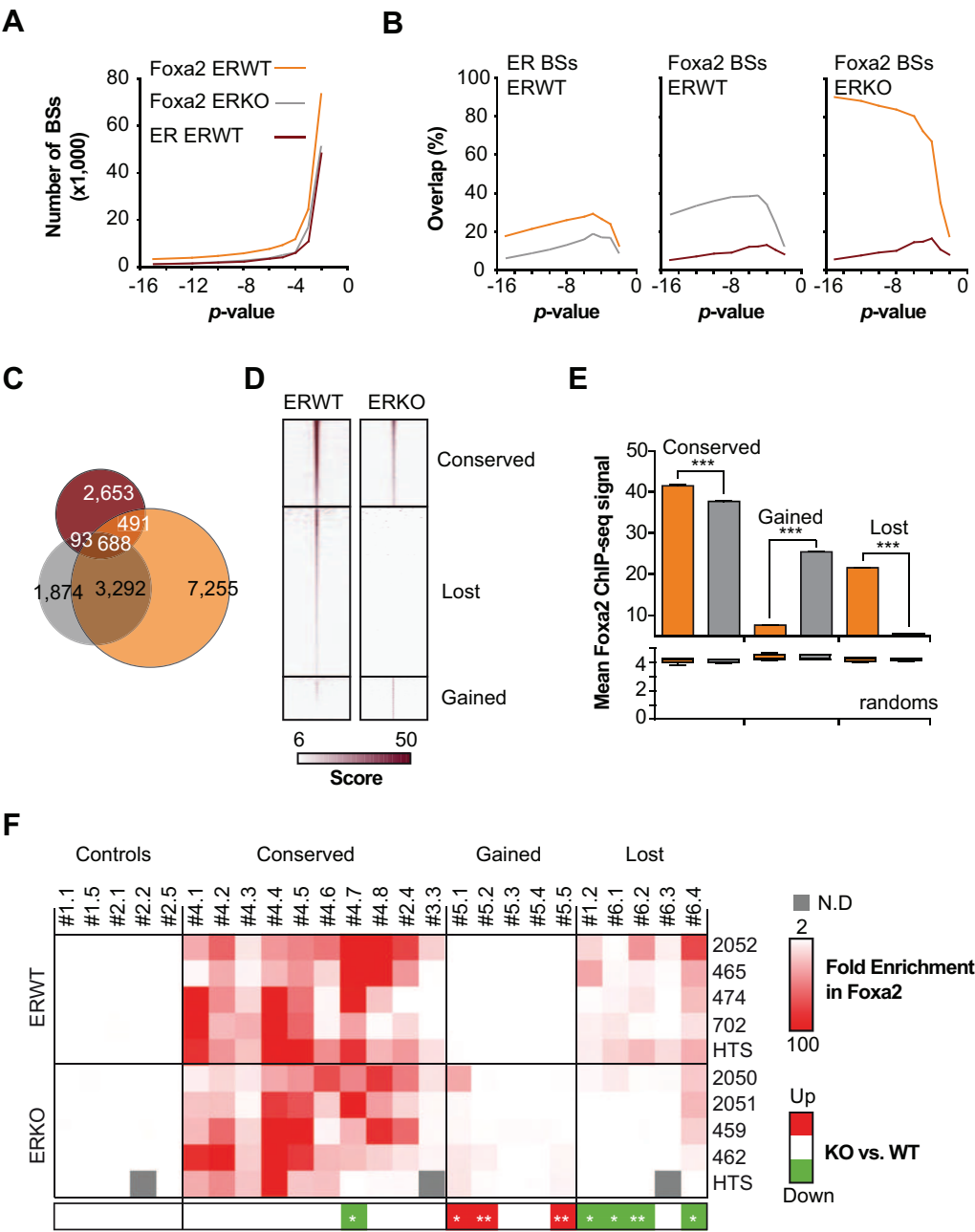
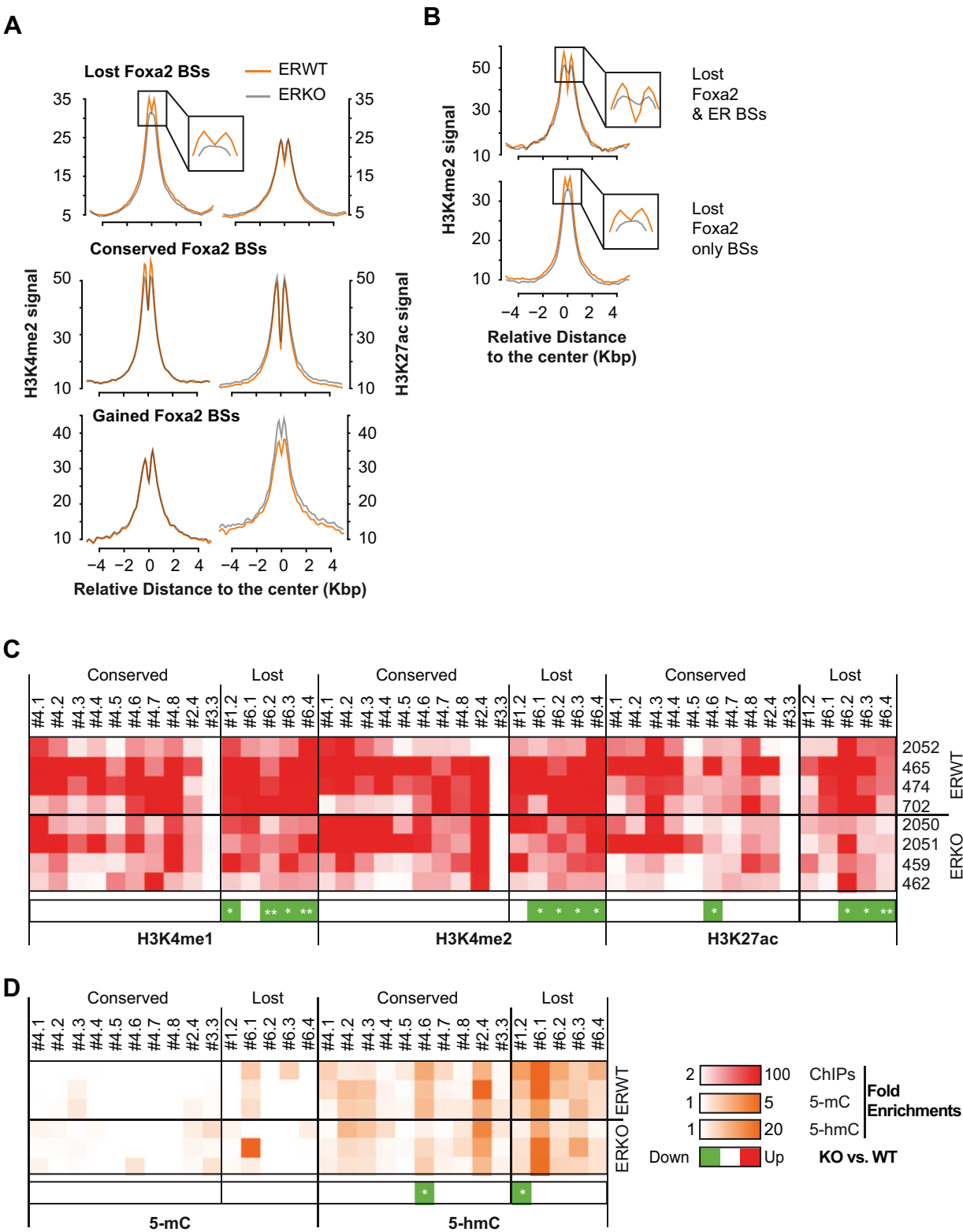


Figure 10



## Figure 11

